Wetterich, S., Schirrmeister, L., Andreev, A. A., Pudenz, M., Plessen, B., Meyer, H., Kunitsky, V. (2009): Eemian and Late Glacial/Holocene palaeoenvironmental records from permafrost sequences at the Dmitry Laptev Strait (NE Siberia, Russia). - Palaeogeography Palaeoclimatology Palaeoecology, 279, 1-2, 73-95

DOI: 10.1016/j.palaeo.2009.05.002

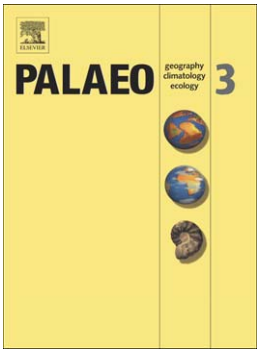

Eemian and Late Glacial/Holocene palaeoenvironmental records from permafrost sequences at the Dmitry Laptev Strait (NE Siberia, Russia)

Sebastian Wetterich, Lutz Schirrmeister, Andrei A. Andreev, Michael Pudenz, Birgit Plessen, Hanno Meyer, Viktor V. Kunitsky

PII: S0031-0182(09)00173-4
DOI: doi: 10.1016/j.palaeo.2009.05.002
Reference: PALAEO 5009

To appear in: *Palaeogeography*

Received date: 10 February 2009
Revised date: 17 April 2009
Accepted date: 1 May 2009

Please cite this article as: Wetterich, Sebastian, Schirrmeister, Lutz, Andreev, Andrei A., Pudenz, Michael, Plessen, Birgit, Meyer, Hanno, Kunitsky, Viktor V., Eemian and Late Glacial/Holocene palaeoenvironmental records from permafrost sequences at the Dmitry Laptev Strait (NE Siberia, Russia), *Palaeogeography* (2009), doi: 10.1016/j.palaeo.2009.05.002

Eemian and Late Glacial/Holocene palaeoenvironmental records from permafrost sequences at the Dmitry Laptev Strait (NE Siberia, Russia)

Sebastian Wetterich[1*], Lutz Schirrmeister[1], Andrei A. Andreev[1], Michael Pudenz[2], Birgit Plessen[3], Hanno Meyer[1] and Viktor V. Kunitsky[4]

(1) Alfred Wegener Institute for Polar and Marine Research, Department of Periglacial Research, Telegrafenberg A43, 14473 Potsdam, Germany; (2) Free University Berlin, Institute of Geological Sciences, Palaeontology Branch, Malteserstrasse 74-100, 12249 Berlin, Germany; (3) Deutsches GeoForschungsZentrum Potsdam, Section 3.3, Telegrafenberg, 14473 Potsdam, Germany; (4) Permafrost Institute, Siberian Branch of the Russian Academy of Sciences, ul. Merzlotnaya, 36, 677010 Yakutsk, Russia

* Corresponding author: sebastian.wetterich@awi.de

Keywords: Late Quaternary, Interglacial, permafrost, palaeoenvironments, Siberia, ostracoda, palynology

Abstract

Terrestrial permafrost sections from the southern and northern coasts of Dmitry Laptev Strait have preserved records of landscape transition from glacial to interglacial periods. They allow geomorphologic and environmental changes to be traced from pre-Eemian time to the Eemian, and from the Late Glacial to the Holocene. The transition from one period to another induced extensive thawing of permafrost (thermokarst). Evolving thermokarst depressions transformed formerly frozen ground into taberal (unfrozen) deposits with accumulating

overlying lacustrine deposits. Lacustrine horizons rich in palaeontological remains retain evidence of changes in environmental conditions. The pollen records reflect changes from grass-sedge dominated vegetation during the Early Eemian to shrub dominated spectra during the Middle Eemian thermal optimum followed by Late Eemian grass-sedge dominated tundra vegetation. Abundant *Larix* pollen have been found in Middle Eemian deposits from the south coast of the Dmitry Laptev Strait (Oyogos Yar), but are absent in similar deposits from the north coast (Bol'shoy Lyakhovsky Island), likely indicating that the northern tree line was located near the Oyogos Yar region during the Eemian thermal optimum. Grass-sedge dominated tundra vegetation occurred during the Late Glacial/Holocene transition which was replaced by shrub tundra during the early Holocene. Rich fossil ostracod records from Eemian and Late Glacial/Holocene lacustrine deposits could be correlated with the Eemian thermal optimum and the Late Glacial Allerød warm period. For both periods, the stable oxygen isotope data from the fossil ostracods suggest an approximate mean summer water temperature range between about 10 and 19 °C in the palaeo-lakes.

1. Introduction

Climate and subsequent environmental changes occurred in northern Eurasia during the Quaternary. Glacial-interglacial cycles certainly exerted an enormous influence on Eurasian periglacial landscapes and ecosystems. The study of palaeoindicators from interglacial periods that are preserved in different palaeoarchives allow to reconstruct ancient environments; such reconstructions are useful for understanding the controls on, interactions between, and effects of climate change and ecosystem response (e.g. Lozhkin and Anderson, 1995; Velichko and Nechaev, 2005; Sirocko et al., 2007). However, although Arctic Eurasia is especially sensitive to current and future climate warming (Symon et al., 2005), interglacial

palaeoenvironmental records from this region are less studied than are those from lower latitudes.

Huge areas of the Eurasian landmass are underlain by permafrost. Permafrost occurrence depends on climate (temperature) conditions, and both past and present climate dynamics influence the state, stability, and distribution of permafrost. One of the most common reactions of periglacial landscapes during interglacial warm periods is extensive thawing of ground ice; this permafrost-degrading process is known as thermokarst. Thermokarst progressively leads to the formation of large-scale, often lake-filled depressions (alases) in the landscape surface and also to the formation of ice wedge casts (pseudomorphs) which are small-scale, secondary sediment-filled depressions (French, 2007).

Both alases and pseudomorphs can be regarded as interglacial palaeoarchives in Northeast Siberia because they contain well-preserved remains such as plant macrofossils (e.g. Kienast et al., 2008), pollen, rhizopods, and chironomids (e.g. Andreev et al., 2004, 2009; Ilyashuk et al., 2006); these remains are useful for palaeoenvironmental reconstructions. In this context, fossil freshwater ostracods are a newly-introduced palaeoindicator for the permafrost archive (Wetterich et al., 2005); their taxonomical-ecological relationships and their geochemistry (stable isotopes) are the primary useful measurements.

The study presented here deals with cryolithological as well as palaeoecological pollen and ostracod records from two Eemian and two Late Glacial/Holocene permafrost sequences exposed on the coasts of the Dmitry Laptev Strait. These records were obtained during the summer 2007 by a joint Russian-German Lena-New Siberian Islands expedition.

2. Regional setting

The Dmitry Laptev Strait connects the Laptev and East Siberian Seas (Figure 1); its coasts have long been of geographical and geological interest. The coastal outcrops along the Dmitry

Laptev Strait are characterised by frozen Quaternary sediments of different ages and accumulation types which are exposed on steep bluffs of thermokarst depressions, thermo-erosional valleys and Yedoma hills which are remnants of late Pleistocene accumulation plains in Northeast Siberian lowlands.

Since its discovery in the 18th century, Bol'shoy Lyakhovsky Island, north of the Dmitry Laptev Strait, has been well-known for the presence of fossil mammal bones; it has become one of the most important Pleistocene mammal sites in Siberia (Chersky, 1891). Permafrost sequences exposed on the south coast of Bol'shoy Lyakhovsky Island were first studied in the 19th century (Bunge, 1887; von Toll, 1897). However, detailed geocryological and palaeoenvironmental studies began much later on both Bol'shoy Lyakhovsky Island (Romanovskii, 1958a-c; Pirumova, 1968; Igarashi et al., 1995; Nagaoka et al., 1995; Arkhangelov et al., 1996; Kunitsky, 1996, 1998; Kunitsky and Grigoriev, 2000) and on the coast of Oyogos Yar, south of Dmitry Laptev Strait (Kayalaynen and Kulakov, 1966; Ivanov, 1972; Gravis, 1978; Konishchev and Kolesnikov, 1981; Vereshchagin, 1982).

The general stratigraphic situation of Quaternary sediments exposed on both coasts of the Dmitry Laptev Strait is similar (Table 1), but the stratigraphy is complicated because absolute age determinations are rare and single stratigraphic units possess different local definitions.

However, such archives including Eemian deposits are generally low studied in the Siberian Arctic (e.g. Allaikha River, Indigirka River lowland, Kaplina et al., 1980; Duvanny Yar, Kolyma River lowland, Kaplina et al., 1978; El'gygytgyn Lake, Chukotka, Lozhkin et al., 2007) and the coastal exposures of the Dmitry Laptev Strait are regarded as the longest and most comprehensive Arctic permafrost archive; it contains records of two to three glacial-interglacial cycles from the middle Pleistocene to the Holocene. Past studies by Russian scientists (e.g. Romanovskii, 1958a-c; Arkhangelov et al., 1996; Kunitsky, 1998; Romanovskii et al., 2000) and joint Russian-German projects (Meyer et al., 2002; Schirrmeister et al., 2002a-c; Andreev et al., 2004, 2009) have described and partly dated

different stratigraphic units of middle and late Quaternary age. Tertiary deposits and weathering crusts, middle Pleistocene ice-rich deposits, and well-sorted loess-like sequences have been found. The permafrost coast along both sides of the Dmitry Laptev Strait is composed of Eemian horizons of lacustrine deposits containing ice wedge casts and late Pleistocene ice-rich deposits of the Yedoma Suite as well as Holocene thermokarst sequences (Table 1).

3. Material and methods

3.1 Field methods and cryolithology

After conducting a survey along the sea coasts, permafrost exposures in coastal bluffs were selected for detailed studies. In general, field studies were difficult due to limited accessibility of the steep permafrost outcrops and extensive mudflows on the slopes. Therefore, composite profiles were obtained which consist of several sub-profiles. Such subprofiles were dug by spades and cleaned with hatchets. The exposed sequences were surveyed, described, photographed, and sketched according to sediment colour, composition, and structures as well as ice structures (cryostructures). Distances, altitudes above sea level (a.s.l.), and depths below surface (b.s.) were gauged using measuring tape. Afterwards, the frozen deposits were taken for further analyses using hammers and small axes and packed in plastic bags. While still in the field, subsamples were placed in sealed aluminium boxes in order to determine the gravimetric (grav.) ice content which is defined as the ratio of ice mass in a sample to the total dry sample mass, expressed as a weight percentage (wt%) (van Everdingen, 1998).

3.2 Geochronology

Selected plant fragments from Late Glacial/Holocene sequences (Figures 5 and 7) were radiocarbon-dated at the Accelerator Mass Spectrometry (AMS) facilities at the Leibniz

Laboratory for Radiometric Dating and Stable Isotope Research (Kiel University, Germany). Conventional ^{14}C ages were calculated according to Stuiver and Polach (1977), with a $\delta^{13}C$ correction for isotopic fractionation based on the $^{13}C/^{12}C$ ratio measured by the AMS system simultaneously with the $^{14}C/^{12}C$ ratio. Calibrated ages were calculated using "CALIB rev 5.01" (Data set: IntCal04; Reimer et al., 2004). The Leibniz Laboratory reduces the background inherent to the spectrometer, which results in low background count rates of the detector, equivalent to an apparent age of 75 kyr (gated background) (Nadeau et al., 1997). Details of the Leibniz Laboratory AMS procedures are given by Nadeau et al. (1997, 1998).

3.3 Sedimentology and stable isotopes

Moist sediment samples were freeze-dried (Christ ALPHA 1-4) in the laboratory, gently manually homogenised, and split into equal parts for the various analyses. In total, 102 samples have been analysed using different methods. A laser particle analyser (Coulter LS 200) was used to measure grain size distribution. Samples were treated with hydrogen peroxide before analysis to successively dissolve organic particles. The mass-specific mineral magnetic susceptibility (MS) was determined using a Bartington MS2 MS meter equipped with an MS2B sensor. The values of mass specific magnetic susceptibility are expressed in SI units (10^{-8} m^3/kg). The contents of total organic carbon (TOC), total carbon (TC), and nitrogen (N) were measured with a Carbon-Nitrogen-Sulphur CNS analyser (Elementar Vario EL III). Stable carbon isotope ratios ($\delta^{13}C$) in TOC were measured with a Finnigan DELTA S coupled to a FLASH element analyser and a CONFLO III gas mix system after removal of carbonate with 10% HCl in Ag-cups and combustion to CO_2. Due to technical difficulties, samples from the Oy7-11 profile were analysed for their $\delta^{13}C$ in TOC using a Finnigan DELTAplusXL mass spectrometer coupled with a Carlo-Erba CN2500 elemental analyser. Accuracy of the methods was determined by parallel analysis of international and internal standard reference materials. The analyses were accurate to ±0.2‰. The $\delta^{13}C$ values are

expressed in delta per mil notation (δ, ‰) relative to the Vienna Pee Dee Belemnite (VPDB) Standard.

Ice wedges from two sections on Bol'shoy Lyakhovsky Island were sampled for stable oxygen ($\delta^{18}O$) and hydrogen (δD) isotopes; the first section was located above an Eemian sequence, and the second section within a Late Glacial/Holocene sequence. Ice screws were used to drill transects across the exposed ice, keeping a distance of 0.1 m between the drill-holes. The ice samples were stored cool and afterwards analysed by equilibration technique with a mass spectrometer (Finnigan MAT Delta-S). The reproducibility derived from long-term standard measurements is established with 1σ better than ±0.1‰ (Meyer et al., 2000). All samples were run at least in duplicate. The values are expressed in delta per mil notation (δ, ‰) relative to the Vienna Standard Mean Ocean Water (VSMOW) Standard.

3.4 Palaeoecological proxies

Pollen

In total, 102 samples were studied for pollen and palynomorphs. A standard hydrofluoric acid HF technique was applied for pollen preparation (Berglund and Ralska-Jasiewiczowa, 1986). Pollen and spores were identified using a microscope (Zeiss Axioskop 2) with 400 x magnification. At least 200 pollen grains were counted in every sample. The relative frequencies of pollen taxa were calculated from the sum of the terrestrial pollen taxa. Spore percentages are based on the sum of pollen and spores. The relative abundances of reworked taxa (Tertiary spores and redeposited Quaternary pollen) are based on the sum of pollen and redeposited taxa, and the percentages of algae are based on the sum of pollen and algae. The Tilia/TiliaGraph/TGView software programs (Grimm, 1991, 2004) were used to calculate percentages and to draw diagrams. Diagrams were zoned by visual inspection.

Freshwater ostracods

For ostracod analyses, sediment samples (ca. 200 g each) were wet-sieved through a 0.25 mm mesh screen, and then air-dried. In total, 102 sediment samples were screened for ostracods. Ostracod valves were found in 47 sediment samples and identified under a stereo-microscope (Zeiss Stemi SV11 Apo). The ostracod taxonomy was based on relevant species descriptions (Alm, 1914; Pietrzeniuk, 1977; Meisch, 2000) following the taxonomy in Meisch (2000). For scanning electron microscopy (SEM) images of fossil ostracod valves we used a Zeiss Gemini Ultra plus at the Deutsches GeoForschungsZentrum Potsdam (German Research Centre for Geosciences Potsdam).

The common species *Candona candida* and *Cytherissa lacustris* from 11 sediment samples in total were prepared for stable isotope analyses. In order to create sufficient material (ca. 50 µg) for isotope analyses for each species we combined three valves of *C. candida* or two valves of *C. lacustris* into one subsample. Altogether, 58 ostracod subsamples were analysed for stable oxygen ($\delta^{18}O$) and carbon ($\delta^{13}C$) isotopes. Usually three subsamples per sediment sample were analysed and afterwards averaged. Following Keatings et al. (2006) the ostracod valves were manually cleaned by removing adhered particles under the binocular microscope using fine brushes and needles. Only clean valves from adult specimens were used for analysis. The prepared valves were dissolved with 103% phosphoric acid and analysed for $\delta^{18}O$ and $\delta^{13}C$ by a mass-spectrometer (Finnigan MAT 253) directly coupled to an automated carbonate preparation device (Kiel IV). The analytical precision as determined by standard measurements (NBS 19) is better than ±0.06‰ (1σ) for $\delta^{18}O$ and ±0.04‰ (1σ) for $\delta^{13}C$. The stable isotope data are expressed in delta per mil notation (δ, ‰) relative to the VPDB standard.

4 Results

4.1 Geochronology and permafrost properties of the Eemian sequences

Geochronology

Eemian deposits were stratigraphically classified according to previously dated and palaeo-ecologically determined interglacial horizons of similar structure and composition in comparable stratigraphic positions (Andreev et al., 2004, 2009; Ilyashuk et al., 2006; Kienast et al., 2008). The most essential lithostratigraphic evidence besides the geochronological and biostratigraphical records is the large-scale coverage of the assumed Eemian deposits by Ice Complex sequences of the late Pleistocene Yedoma Suite.

Eemian exposure on the south coast of Bol'shoy Lyakhovsky Island (L7-14)

On Bol'shoy Lyakhovsky Island a section within an ice wedge cast, filled with alternating beds of peaty brownish plant detritus layers and grey clayish silt layers, was studied (subprofiles B and C; Figure 2a, b, e). Ripple bedding (ripples 1-2 cm high, 2-5 cm spacing), fine laminated layers (each lamination 5-10 mm thick), and small-scale synsedimentary slumping structures were common (Figure 2e). Several layers contained mollusc shells, about 5 mm in diameter. Larger twig fragments and peat inclusions of 2-3 cm in diameter were also observed. The cryostructure was predominantly massive. Only single thin ice veins (< 1 mm thick) were visible parallel to the bedding.

The ice wedge cast was underlain by grey silt (subprofile A; Figure 2a, b, e) with irregular fine single white laminations (< 1 mm thick). No plant remains were observed, but numerous small, dark-grey round spots, probably decomposed plant remains, were visible. The cryostructure was massive. This material represents thawed and refrozen (taberal) deposits.

The alternate bedding structures of the ice wedge cast were discordantly covered by ice-rich deposits (subprofile D, E and F; Figure 2a, b, d). This sequence exposed the transition

between laminated lacustrine and weakly-bedded ice-rich boggy deposits. The latter were characterised by lens-like cryostructures, ice bands (Figure 2d), and the occurrence of single twig fragments. The ice-rich sequence of silty sand transformed gradually into a thick peat horizon.

The transition horizon contained several large peat inclusions ≈30 cm in diameter. The cryostructure was banded (2-5 cm thick bands) with coarse lens-like reticulations between ice bands, reflecting conditions of ice supersaturation. Several vertical ice veins (1 to 1.5 cm broad, 20 cm long) were observed in 20 cm distance to each other in the upper part of the peat horizon. The entire sequence was framed by ≈1 m wide ice wedges to the left and to the right, and is considered to be polygon filling (Figures 2a, c). The peat horizon consisted of numerous large peat lenses embedded in greyish sandy silt. Similar thick peaty horizons were observed at several other places on the coast. Therefore, it can be concluded that the sequence of interglacial finely-laminated lake deposits covered by ice-rich silty sands and a peat layer is of stratigraphic importance. Further upwards to the surface the coastal section consisted of a ≈20 m thick Ice Complex sequence. According to grain size analysis, the studied deposits are poorly sorted clayish sandy silts (Figure 3). The silt fraction is dominant, but the changing content of fine-grained and middle-grained sand reflects the alternating beds of lacustrine Eemian deposits. The sedimentological records of the well-bedded part and the adjacent underlying and covering layers are similar. Therefore, both the underlying and overlying layers seem to have been transformed by thawing and freezing or by refreezing only after accumulation. In general, two horizons could be distinguished. The lower horizon containing less ice and organic carbon corresponds to the Eemian lacustrine sequence. The upper horizon of higher ice (100-300 wt%) and TOC contents is considered to be a boggy formation. The $\delta^{13}C$ record probably reflects changes in plant associations which would result from a gradual transition from aquatic to boggy environmental conditions (Figure 3).

Eemian exposure on the coast of Oyogos Yar (Oy7-08)

A second ice wedge cast profile studied on the Oyogos Yar coast was part of a 28 m long coastal section mostly composed of late Pleistocene Ice Complex deposits (Schirrmeister et al., 2009). For this paper, we selected the lower two subprofiles A and B underlying the Ice Complex deposits (Figure 4a). Subprofiles A and B were exposed between 2 and 6 m a.s.l. at the cliff wall of the thermo-terrace to the sea and in a small thermo-erosional gully cutting the thermo-terrace (Figure 4b).

The lowest horizon (sample Oy7-08-01 of subprofile A) underlying the ice wedge cast contained grey taberal deposits with black spots and several plant remains. The cryostructure was massive. These deposits were covered by light-brown peat lenses (2 x 5 to 10 x 15 cm) in a grey sandy silt matrix with lens-like reticulated cryostructure and higher ice content. In addition, single ice lenses 5 mm thick were visible. Disturbed layering and white lines of thaw structures between the layers were observed. The lowermost layer of the exposed ice wedge cast consisted of finely-laminated 1-2 to 5-10 mm thick alternating layers of brownish plant detritus layers and grey sandy silt layers (Figure 4a). The cryostructure was fine lens-like reticulated.

The centre of the ice wedge cast and the overlying deposits were studied in the second subprofile B (Figure 4a). This subprofile was composed of numerous 5-10 cm thick alternating plant detritus layers and sandy silt layers (Figure 4c). Ripple bedding, synsedimentary slumping structures, and separate peat lenses were observable in some layers. The cryostructure was lens-like layered. Ice lenses were oriented parallel to the bedding. Further upwards the bedding was disturbed and the plant detritus content decreased. Grey silty sand dominated this horizon, which contained numerous mollusc shells. The cryostructure changed upward from lens-like layered to lens-like reticulated. Because of overlapping sample heights the analytical records of subprofile A were presented separately in Figure 4. The entire sequence consisted of less-sorted clayish sandy silt. Small-scale changes

of mean grain size and of sand fraction reflect the alternating bedding of the lacustrine deposits. The horizon below the ice wedge cast is characterised by $\delta^{13}C$ values lighter than those of the ice wedge cast sediments (Figure 3).

4.2 Geochronology and permafrost properties of the Late Glacial/Holocene sequences

Geochronology

In total, the plant remains and detritus in twenty sediment samples from both Late Glacial/Holocene sequences have been radiocarbon dated (Table 2).

The age-height relationship is not consistent, probably due to pre-sedimentary relocation and post-sedimentary cryogenic processes. Furthermore, the interpretation of the stratification is complicated by the sampling of subprofiles at different positions. However, the general picture is similar at both study sites on the northern and southern coasts of the Dmitry Laptev Strait. Late Pleistocene taberal deposits dated between about 46.6 and 36.6 kyr BP are discordantly overlain by lake deposits dated from about 11.8 to 7.1 kyr BP at the Bol'shoy Lyakhovsky section (profile L7-08) and from about 14.8 to 10.7 kyr BP at the Oyogos Yar section (profile Oy7-11). The overlying boggy deposits accumulated from about 7.5 to 4.0 kyr BP at the Bol'shoy Lyakhovsky section and between about 10.0 and 3.3 kyr BP at the Oyogos Yar section. The late Holocene deposits discordantly cover the underlying older Holocene sediments.

Alas exposures on the south coast of Bol'shoy Lyakhovsky Island (L7-08, R33-A1)

An 8 m thick sediment sequence in the centre of a thermokarst depression, cut by the coastal cliff, was studied about 4.1 km west of the Zimov'e River mouth (Figure 1).

The lowermost exposed horizon consisted of greenish grey sandy silt, the thawed and refrozen (taberal) remains of Ice Complex deposits (Yedoma Suite), containing peat lenses of 5-10 cm length (Figure 5).

The cryostructure was coarse lens-like reticulated. The gravimetric ice content was relatively low. Above this horizon, a 0.5 m thick layer of cryoturbated peaty palaeosol containing less-decomposed, light-brown peat moss and a dark-brown peat layer with wood fragments in a sandy silt matrix was exposed. The cryostructure was net-like to lens-like, with 4-5 cm long ice lenses, and an ice content of 38 to 46 wt%. This segment was covered by 4 m of lacustrine deposits altogether, consisting of alternating beds of dark-grey clayish silt and 2 mm thick dark-grey layers of plant detritus. The cryostructure was lattice-like with distances between separate ice veins of 5-10 cm. This part was additionally marked by 2 to 3 cm thick brownish zones of iron oxide impregnations along cracks. The uppermost 3 m of the alas sequence were characterised by light-brown, 10 to 15 cm long peat inclusions in light-grey sandy silt matrix reflecting subaerial accumulation conditions. The cryostructure was banded and lens-like between ice bands. Between 1.1 to 0.3 m below the surface grass roots and peat layers occurred. The cryostructure consisted of diagonally-ordered, partly-broken ice veins and lenses, or of lattice-like structures. The studied deposits from the L7-08 sequence are predominantly composed of less-sorted fine-grained sand. Three horizons (taberal, lacustrine, boggy) were separated according to sedimentological, biogeochemical, and cryolithological results (Figure 6).

The bedding of the lacustrine segment is reflected in changing mean grain size values and variations in the silt and sand fractions. The less variable magnetic susceptibility reflects the homogenous mineral composition of these deposits. Taberal Ice Complex deposits below and boggy deposits above the lacustrine horizon are clearly separated by lighter $\delta^{13}C$ values (< −30‰), higher TOC contents, and low values of magnetic susceptibility.

An additional alas section (R33) already described by Andreev et al. (2009) exposed on the eastern slope of the same thermokarst depression was additionally used for ostracod studies. The cryolithological and stratigraphic situation was generally similar to that of the above-mentioned section. According to radiocarbon data, the lower horizon was formed during the

Middle Weichselian. The upper subaquatic and the subaerial sediments containing molluscs, snails, and thin layers with leaves, accumulated between 12 and 8 ^{14}C kyr BP. The sequence was covered by boggy deposits that are 3.7 kyr BP old. Woody remains were radiocarbon dated between 8.4 and 8.9 kyr BP and found in a near-surface ice wedge cast (Andreev et al., 2009).

Alas exposure on the coast of Oyogos Yar (Oy7-11)

This exposure consists of two subprofiles that were studied at the coast on both sides of an erosional crack (Figure 7a).

The sediment sequence was exposed at an ≈ 10 m high wall, where subprofile A was studied, and at a fallen block opposite to the wall, where subprofile B was accessible. The lower subprofile A (Figure 7a) consists of taberal Ice Complex deposits of the Yedoma Suite.

The light-grey silty sand contained no or rare visible plant detritus. The cryostructure was lens-like layered. One mm thick, 5-15 cm long ice lenses occurred 1-2 cm apart. Irregular white lines were also observed and were interpreted as thaw structures. These whitish structures occurred with increasing frequency closer to the overlaying peaty soil. This palaeosol layer contained twigs and peat inclusions. Above this buried soil, lacustrine deposits were indicated by alternating layers of silty fine sand and plant detritus. Ripple marks, small faults, wood fragments, and mollusc shells were observed. The cryostructure was lens-like layered. Similar lacustrine sediments were found in a flanking ice wedge cast (Figure 7c). Small epigenetic ice wedges became a broad syngenetic ice wedge crossing the sediment sequence, similar to the above-described section on Bol'shoy Lyakhovsky Island.

The lake sequence was covered by a peat horizon which was not accessible in subprofile A. Therefore, the upper part of the alas sequence was studied in a separate block directly in front of the wall (Figure 7b). The 20 to 30 cm thick peat horizon was dense and platy and contained wood fragments (2-3 cm in diameter) and 1-2 mm thick silt layers. Further upward, greyish

silty sand and light-brown peat lenses were found. The cryostructure was banded and coarse lens-like reticulated. Ice lenses up to 1 cm thickness were composed of vertical ice needles.

Field observations indicated that the alas sequence was subdivided into three different parts; this conclusion was confirmed by analytical records (Figure 6). The entire sequence predominantly consists of poorly sorted silt. The lowermost taberal Ice Complex deposits are characterised by fine-grained clayish silt. The covering lacustrine segment contains more sand. The magnetic susceptibility of both parts was similar (about 30 x 10^{-8} m^3/kg) reflecting a similar sediment source. The observed bedding of lacustrine sediments is shown by variations in mean grain size. Finally, the uppermost boggy segment is characterised by higher ice content, lower mean grain size, and variations in magnetic susceptibility and TOC values.

4.3 Stable isotope ground ice records

Stable isotope data from ice wedges presented here were obtained on Bol'shoy Lyakhovsky Island. Corresponding samples were taken on Oyogos Yar; those analyses are still in progress and the subject of an upcoming paper by Opel et al. (submitted). We obtained four samples at 8.5 m a.s.l. from a syngenetic ice wedge exposed at section L7-14 above the Eemian lacustrine sediments (Figure 2).

Syngenetic ground ice formed concurrently with sediment accumulation. The isotopic record shows values of ≈ −29‰ for $\delta^{18}O$ and −218‰ for δD, which are relatively light isotopically when compared to the Holocene records of section L7-08. The deuterium (*d*) excess averages about 10.7 (Figure 8, Table 3).

The Holocene stable isotope ground ice record comes from two samples taken at 6.3 m a.s.l. from the epigenetic part and 11 samples at 11 m a.s.l. from the syngenetic part of the Holocene ice wedges exposed at section L7-08 (Figure 5). The epigenetic part formed after sedimentation in the underlying lacustrine deposits, and the syngenetic part formed

approximately simultaneously during sediment accumulation in the boggy deposits (Figure 5). The isotopic records of the Holocene syngenetic ice wedge show heavier values of around −24‰ for $\delta^{18}O$ and −182‰ for δD than the post-Eemian Glacial records of section L7-14. The d excess averages about 7.3 (Figure 8, Table 3). The $\delta^{18}O$ and δD values of the sampled epigenetic parts of the Holocene ice wedges were heavier than those of the syngenetic parts; about −20‰ for $\delta^{18}O$ and −158‰ for δD, an a deuterium excess of around 0.5 (Figure 8, Table 3). The latter value points to interactions between the thin epigenetic parts of ice wedges and the surrounding frozen sediments, altering the primary meteoric precipitation signal.

4.4 Pollen studies of the Eemian sequences

Eemian pollen record from Bol'shoy Lyakhovsky Island

The lowermost spectra (pollen zone I: PZ I) in profile L7-14 (Figure 9) are dominated by pollen of Poaceae and Cyperaceae with some *Betula* sect. *Nanae* and *Alnus fruticosa*. The pollen concentration is low. PZ I contains high numbers of *Glomus* spores (indicative of denudated soils) and reworked ancient (mineralised) Pinaceae. It is also likely that *Pinus* and *Picea* pollen found in PZ I have been reworked as well. Therefore, the pollen spectra of PZ I should be considered carefully. Poaceae and Cyperaceae pollen and *Glomus* spores were probably mostly produced by local vegetation during sedimentation, while numerous coniferous pollen were reworked from older sediments. *Betula* and *Alnus* pollen might also be of reworked or contaminated origin. Taking this into consideration, we should exclude the PZ I spectra from palaeoecological interpretation.

Pollen spectra from PZ II are dominated by pollen from Poaceae, Cyperaceae, *Betula* sect. *Nanae*, and *Alnus fruticosa*. These spectra also contain rather high amounts of *Salix* and *Artemisia* pollen, spores of fungi (dung-inhabiting Sordariales and *Glomus*), and remains of green algae colonies (*Pediastrum* and *Botryoccous*). According to pollen spectra the area

around a supposed initial thermokarst lake was dominated by shrubby tundra vegetation. Climate conditions were relatively moderate (warm and moist).

Pollen spectra from PZ III are mainly composed of pollen from Poaceae, Cyperaceae, *Betula* sect. *Nanae*, and *Alnus fruticosa*. This zone can be subdivided into two subzones. The contents of shrub pollen are the highest in PZ IIIa, reflecting the warmest interval. The remains of green algae colonies and fungal spores are completely absent in the PZ IIIb zone, reflecting dryer local environmental conditions. Lower contents of shrub pollen in the upper subzone also point to a slight cooling.

Eemian pollen record from Oyogos Yar

The pollen concentration of the lowermost sample (PZ I of section Oy7-08) is low (Figure 10). As in the samples from PZ I of section L7-14, it contains relatively high amounts of reworked ancient (mineralised) coniferous pollen (*Larix*, *Pinus*, *Picea*), and is therefore of minor relevance for palaeoecological interpretation. However, some taxa from PZ I can be used to characterise environmental conditions in the area during sedimentation. For example, rather high amounts of Cichoriaceae pollen and *Riccia* spores are notable in the spectrum. Both taxa are indicative of denuded soils and may reflect an unstable environment connected with melting Saalian ice wedges and initial formation of Eemian thermokarst depressions. It is also notable that the Poaceae, Cyperaceae, and *Betula* sect. *Nanae* pollen in PZ I are very similar to pollen types in the lower part of PZ II, and probably reflect similar vegetation around the site. Pollen spectra of PZ II dominated by Poaceae, Cyperaceae, *Larix* and *Betula* sect. *Nanae* pollen (Figure 10) can be subdivided into two subzones. PZ IIa contains higher amounts of *Salix* and *Artemisia* pollen and spores of dung-inhabiting Sordariales fungi (*Sporormiella*, *Podospora*, *Sordaria*), while PZ IIb contains more pollen of *Betula* sect. *Nanae*, *B.* sect. *Albae*, and *Alnus fruticosa*. Rather high amounts of *Larix* pollen in PZ II indicate that larch grew around the study site. Shrub alder and dwarf birch stands were also

common. Very high amounts of *Salix* pollen in the lowermost sample of PZ II may reflect a predominance of willow shrubs in the pioneer vegetation around the site. Relatively high amounts of dung-inhabiting fungal spores in the PZ IIa subzone indirectly point to the presence of grazing herds in the area during the interval between PZ 11a and PZ 11b.

The PZ IIb Oy7-08-05 and -06 samples from subprofile Oy7-08-A correlate with the samples Oy7-08-07 and -17 from the subprofile Oy7-08-B that was sampled in detail; at Oy7-08-B the record continues as PZ III of subprofile Oy7-08-B (Figure 10).

PZ III is dominated by pollen of Poaceae, Cyperaceae, *Betula* sect. *Nanae*, *Alnus fruticosa*, *Larix*, and spores of *Equisetum* and fungi. The pollen spectra of PZ III can be subdivided into two subzones (Figure 10). PZ IIIa differ from PZ IIIb because higher amounts of fungal spores (dung-inhabiting Sordariaceae and *Glomus*) are present in PZ llla, while the numbers of *Larix*, *Salix,* and *Picea* pollen are higher in PZ IIIb. PZ III pollen assemblages reveal a larch forest, with alder shrub and dwarf birch stands dominating the vegetation (Figure 10). The content of *Glomus* spores, which indicate disturbed soils, shows a trend similar to that of the Sordariaceae (especially with *Sporormiella*) and likely indicates the presence of numerous grazing animals during this interval. The highest presence of larch and spruce pollen occurs in PZ IIIb, indicating the most favourable conditions during the Eemian, i.e. the Middle Eemian thermal optimum. Slightly higher numbers of *Salix* pollen and remains of green algae colonies (*Botryococcus* and *Pediastrum*) point to a wetter environment than during the PZ IIIa interval. Numbers of *Larix*, *Salix,* and *Picea* pollen are significantly lower in PZ IV, indicating climate deterioration. Disappearance of dung-inhabiting fungi spores indirectly shows that the number of grazing animals in the area was significantly reduced.

4.5 Pollen studies of the Late Glacial/Holocene sequences

Late Glacial/Holocene pollen record from Bol'shoy Lyakhovsky Island (L7-08)

The pollen spectra of PZ I are mostly dominated by Poaceae and Cyperaceae with few Asteraceae and *Artemisia* (Figure 11). Two radiocarbon dates within PZ I of about 46.6 and 44.0 kyr BP show that the sediments were accumulated during the Middle Weichselian. Similar pollen spectra reflecting open steppe- and tundra-like vegetation are known from the area (Andreev et al., 2009). The presence of shrub pollen (especially *Salix*) might reflect a growth of shrub communities in the area.

PZ II is dominated by Poaceae and Cyperaceae, but also contains rather large numbers of *Betula* sect. *Nanae*, *B.* sect. *Albae,* and *Alnus fruticosa* (Figure 11). According to the radiocarbon dates (Table 2) the sediments were accumulated during the Allerød and the early Holocene. Comparing the studied spectra with other local records (Andreev et al., 2009) shows that these spectra are typical of early Holocene records, but they also contain organic material of different origins due to reworking by thawing and refreezing, and therefore should be interpreted very carefully.

The pollen spectra of PZ III are also dominated by Poaceae and Cyperaceae and contain relatively high amounts of *Betula* sect. *Nanae*, *B.* sect. *Albae* and *Alnus fruticosa* (Figure 11). However, radiocarbon dates from the low part of the section (Table 2) show that sediment is contaminated by older organic matter. The upper part of the sediments (PZ IIIb pollen subzone) was accumulated under wetter conditions as evident by higher amounts of Cyperaceae and green algae colonies remains.

Late Glacial/Holocene pollen record from Oyogos Yar (Oy7-11)

The lowermost PZ I is dominated by Poaceae and Cyperaceae, but also contains large numbers of *Betula* sect. *Nanae*, *B.* sect. *Albae,* and *Alnus fruticosa* (Figure 12).

In addition, the uppermost pollen spectra of PZ I (sample Oy7-11-03) contain a large amount of Sordariaceae fungi spores. Two radiocarbon dates within PZ I of about 41.3 and 36.6 kyr BP (Table 2) show that the sediments accumulated during the Middle Weichselian period.

However, the taberal sediments representing PZ I could have been contaminated by organic material of a different origin due to reworking by thawing and refreezing, and therefore should be interpreted carefully.

The pollen spectra of PZ II are mostly dominated by Poaceae pollen with some pollen from Cyperaceae, *Artemisia*, *Betula* sect. *Nanae,* and a few other taxa. PZ II can be subdivided into two subzones (Figure 12). PZ IIa contains higher numbers of shrub and tree pollen, while PZ IIb shows higher numbers of Asteraceae and spores of fungi. According to the radiocarbon dates (Table 2) PZ IIa spectra indicate a relatively warm interval which might be correlated with the Allerød. PZ IIb spectra indicate some climate deterioration which occurred during the Younger Dryas.

PZ III is characterised by large numbers of shrub and tree pollen reflecting the shrubby tundra vegetation around the site (Figure 12). The radiocarbon dates (Table 2) show the early Holocene age of the sediments. The environmental conditions were warmer than today, corresponding to the Holocene thermal optimum.

PZ IV spectra reflect some climate deterioration that occurred during the late Holocene at about 3.3 kyr BP. However, the climate was still warmer than today and shrubs (*Betula* sect. *Nanae* and *Alnus fruticosa*) grew at a location where no shrubs grow today. The uppermost pollen spectrum is dominated by Poaceae with some Cyperaceae and *Betula* sect. *Nanae,* reflecting a further deterioration. However, the climate was still warmer than today as evidenced by high pollen numbers of *B.* sect. *Nanae* which is not present in the area nowadays.

4.6 Ostracod studies of the Eemian sequences

Associations and ecology

Remains of ostracods have been found in most of the lacustrine sediment samples of Eemian sequences (Figure 13). Taberal deposits situated below the lacustrine sediments generally lack

ostracods, but in the overlying zone of section L7-14 which represents a transition from a lacustrine to a boggy milieu a rich ostracod fauna has been observed.

Changing abundances of ostracods are obvious for several time slices within the record. Especially at the bottom of the lacustrine sediments, ostracods are found rarely or not at all in sediment samples, most likely due to unstable conditions during the early stages of thermokarst lake formation. However, also within the lacustrine sediments but further upwards, the ostracod record is inconsistent, probably indicating periods of desiccation or other changes in the aquatic regime. A total of 14 Eemian ostracod species was identified (Figure 14, Table 4). The species composition differs between the deposits from Bol'shoy Lyakhovsky Island and Oyogos Yar coast since the abundance of each species differs between the sites. For example, *Limnocythere falcata* is very common in deposits from Oyogos Yar, but rare on Bol'shoy Lyakhovsky Island while *L. suessenbornensis* and *Cypria exsculpta* are generally lacking on Bol'shoy Lyakhovsky Island. The three species *L. falcata*, *L. suessenbornensis,* and *Eucypris dulcifons* from the Eemian sequences are not reported from modern environments, but are known from middle to late Pleistocene deposits in Germany (Diebel, 1968; Diebel and Pietrzeniuk, 1969). Common species from both coastal exposure sites are *Candona candida*, *Fabaeformiscandona levanderi*, *F. rawsoni*, *Limnocytherina sanctipatricii* and *Ilyocypris lacustris*. The modern ecological requirements of these species are not very specific since these species are tolerant to temperature and salinity variations. *C. candida* and *F. rawsoni* are known from modern thermokarst lakes in Central Yakutia (Wetterich et al., 2008a) and *L. sanctipatricii* from polygon ponds in North Yakutia (Wetterich et al., 2008b).

Stable isotopes

The stable isotope record of ostracod calcite from the Eemian period was analysed in samples from section Oy7-08 (Table 5). The mean $\delta^{18}O$ record of *C. candida* during this period ranges

from −11.3 to −12.6‰, while the record of species *C. lacustris* varies from −12.2 to −14.5‰ (Table 5).

The difference of > 1‰ between the mean values of the two species is probably due to species-dependent metabolic (vital) offsets. Such an effect leads to ^{18}O-enrichment, compared to the precipitation of calcite when isotopes are in equilibrium with the lake water (Hammarlund et al., 1999). The vital offset of *Candona candida* was quantified as 2.1 ± 0.2‰ by von Grafenstein et al. (1999) and as +2.5 to +3‰ by Keatings et al. (2002), whereas the vital offset of *Cytherissa lacustris* is lower at 1.2 ± 0.3‰ (von Grafenstein et al., 1999). The δ^{13}C values range from −4.7 to −5.5‰ for *C. candida* and from −7.3 to −10.2‰ for *C. lacustris* (Table 5).

4.7 Ostracod studies of the Late Glacial/Holocene sequences

Associations and ecology

In sediments from the Late Glacial/Holocene L7-08 and R33 A1 sections on Bol'shoy Lyakhovsky Island, ostracods were found in the lacustrine horizon and in the lower part of the boggy horizon. SEM images of fossil ostracod species are given in Figure 13. In total, 11 species have been identified of which *Candona candida*, *Fabaeformiscandona levanderi*, *Cytherissa lacustris,* and *Cypria exsculpta* were the most abundant (Figure 15, Table 4).

In contrast, the Oyogos Yar Oy7-11 section provided a very poor ostracod record; it included a single valve of juvenile Candoninae in the lowermost taberal deposits, and low numbers of *F. levanderi*, *F. rawsoni,* and *L. falcata* in the overlying lacustrine sediments from the Late Glacial age (Figure 15). As in the Eemian records, changing abundances of ostracods are obvious in several time slices. During the transition from the Late Glacial to the early Holocene, the highest numbers of ostracod remains are seen at about 12.5 kyr BP (samples R33 A1-12 to -15) and at about 11.6 to 10.1 kyr BP (samples L7-08-18 to -20). Such data point to the occurrence of well-developed thermokarst lakes and stable aquatic conditions

even before the beginning of the Holocene. Compared to the Eemian records, the modern ecological demands of the most common species in the Late Glacial/Holocene records do not allow differentiation of aquatic conditions; these species are generalists, preferring cold water and tolerating slightly salty conditions. However, except for *Candona candida* the dominant species from the Late Glacial/Holocene record are absent from modern Central Yakutian thermokarst environments (Pietrzeniuk, 1977; Wetterich et al., 2008a) probably due to generally warmer water temperatures today.

Stable isotopes

A stable isotope record of ostracod calcite from the Late Glacial/Holocene period was obtained from samples of sections L7-08 and R33 A1, and dated from 12.5 to 10.1 kyr BP (Table 5). The $\delta^{18}O$ record of *C. candida* during this period ranges from −12.2 to −15.1‰, and the record of *C. lacustris* ranges from to −12.8 to −14.9‰ (Table 5). As in the Eemian stable isotope record, a general shift of about 1‰ between the mean values of the two species has been observed, likely resulting from different species-dependent vital offsets. The $\delta^{13}C$ values range from −4.2 to −7.4‰ for *C. candida* and from −6.0 to −9.9‰ for *C. lacustris* (Table 5).

5. Discussion and interpretation

5.1 Local palaeoenvironmental changes during the Eemian

The lithostratigraphical structure of the Eemian sections at the northern and southern coast of Dmitry Laptev Strait show a similar general pattern of three different horizons which accumulated under different environmental conditions.

The lowermost sequences of taberal deposits represent thawed and subsequently refrozen material which likely accumulated in pre-Eemian times and underwent thawing during the

Eemian Interglacial when thermokarst processes led to the formation of lakes and thawed deposits (taliks) below the lakes.

The sedimentological and cryolithological features of the pre-Eemian taberal horizons show single whitish laminations which are interpreted as thaw signs, numerous small dark-grey spots representing strongly decomposed organic matter, and a massive cryostructure. The pollen records (lowermost PZ I of L7-14 and Oy7-08) reveal relatively high amounts of reworked ancient (mineralised) coniferous pollen, and ostracod remains are absent. Similar results were obtained in formerly described pre-Eemian deposits of Bol'shoy Lyakhovsky Island (Andreev et al., 2004).

The refreezing of the taberal horizons took place in post-Eemian time and the deposits remained frozen until today. Such taberal deposits are covered by the Eemian lacustrine sequence that formed due to warmer conditions during the Interglacial when thermokarst lakes occurred. Under such conditions pre-Eemian ice wedges thawed; at their positions small thermokarst lake basins formed and lacustrine sediments began to accumulate. Distinctive features of the lacustrine sediments are the alternating beds of finely laminated brownish plant detritus and grey sandy silt layers.

The Eemian pollen records (PZ II and III) from both locations show similarities reflecting comparable vegetation. The main difference between the Bol'shoy Lyakhovsky and Oyogos Yar Eemian pollen records is the absence of *Larix* at the northern location. The northern tree line likely reached the Oyogos Yar region during the Middle Eemian, but not the Bol'shoy Lyakhovsky region. Basing on correlation of the studied pollen assemblages with previously studied records (Andreev et al., 2004; Ilyashuk et al., 2006; Kienast et al., 2008) we may assume that the PZ II of L7-14 and Oy7-08 represents the Early to Middle Eemian period. High numbers of *Glomus* spores indicate that vegetation and soils were significantly disturbed, probably due to active erosion processes connected with the melting of Saalian ice wedges and thermokarst lake formation. Rather high numbers of *Artemisia* and the presence

of herb pollen taxa such as Brassicaceae, Caryophyllaceae, and Asteraceae show that open plant associations were also common. Dung-inhabiting fungi spores in the pollen spectra indirectly point to the presence of grazing animals around the lake. PZ IIIa (Oy7-08-B) was formed during the Middle Eemian thermal optimum. Climate conditions in the Eemian were warmer than today in northern Yakutia as has already been discussed on the basis of pollen and plant macrofossil data from exposures on Bol'shoy Lyakhovsky Island. Andreev et al. (2004) provided a quantitative climate reconstruction based on a pollen-climate reference data set from northern Eurasia (Tarasov et al., 2005). Mean air temperatures of the warmest month (MTWA) vary from 7.8 to 9.6 °C for the Eemian thermal optimum (modern MTWA at Cape Shalaurova, Bol'shoy Lyakhovsky Island: 2.8 °C; Rivas-Martínez, 2007). Using Eemian plant macrofossil records from Bol'shoy Lyakhovsky Island, Kienast et al. (2008) concluded a MTWA of about 12.5 °C for the Eemian optimum. The pollen spectra of PZ IIIb (Oy7-08-B) indicate gradual climate deterioration during the Late Eemian.

The occurrence of numerous well-preserved ostracod remains in the lacustrine horizons points to stable aquatic conditions due to extensive thawing of pre-Eemian permafrost deposits and the widespread occurrence of thermokarst lakes caused by generally warmer climate conditions. The Eemian ostracod assemblages are dominated by species which tolerate the considerable changes in temperature and salinity regimes that are typical of modern habitats like thermokarst lakes and polygon ponds in the periglacial landscapes of East Siberia.

The Eemian lacustrine deposits are discordantly covered by thick Ice Complex deposits (Yedoma Suite) of late Pleistocene age.

5.2 Local palaeoenvironmental changes during the Late Glacial/Holocene

As already described for the Eemian sequences, the Late Glacial/Holocene sedimentological records are also subdivided into taberal, lacustrine, and boggy deposits. The accumulation record of this period based on available radiocarbon dates is not consistent (Table 2). Middle

Holocene deposits from about 7.5 to 4.0 kyr BP have not been found in the Dmitry Laptev Strait exposure. Similar situations are known from other key regional Quaternary sections of permafrost deposits (Schirrmeister et al., 2002b, c, 2003, 2008; Sher et al., 2005; Andreev et al., 2009). Thermokarst-related landscape dynamics during interglacial or interstadial warm periods led to extensive melting and reworking of underlying ice-rich deposits, and such processes are likely responsible for the lack of sediment preservation. Low sedimentation rates during the middle Holocene are another possible explanation that to date remains unsubstantiated. Generally, Late Glacial and Holocene deposits mostly appear in the permafrost region of northern Yakutia as filling of thermokarst depressions or as a thin horizon above late Pleistocene sequences. The studied sequences exhibit a sedimentation history in which late Pleistocene Ice Complex deposits dated from about 46.6 to 36.6 kyr BP are discordantly overlain by Late Glacial deposits dated to 14.8 kyr BP and younger. The boundary between the two sequences is visually obvious due to exposure characteristics, and is also distinguished by differences in sedimentological and cryolithological properties. The lowermost sequence is built up of taberal deposits of the former Ice Complex, composed of sandy silt containing peat lenses and thaw signs (whitish laminations) and lens-like reticulated or layered cryostructures with generally low ice content. The pollen data from the taberal horizons point to a Middle Weichselian interstadial vegetation. Due to reworking during thawing and refreezing of the deposits, the possibility of pollen contamination cannot be excluded and therefore the taberal horizon is of minor relevance for the palaeoenvironmental interpretation. Ostracods have very rarely been observed in the taberal deposits, but their occurrence in undisturbed Middle Weichselian Ice Complex sequences has been reported by Wetterich et al. (2005, 2008c).

The taberal horizon is discordantly covered by a lacustrine horizon of Late Glacial/Holocene age. Its lowermost part is composed of cryoturbated peaty palaeosols in both sections on the northern and southern coasts of the Dmitry Laptev Strait. The overlying lacustrine horizons of

alternating beds of clayish silts and plant detritus layers are of lens-like or lens-like layered cryostructure and contain mollusc shells, ostracods, and wood fragments.

Radiocarbon dates of single samples and a comparison with previously studied regional records (Grosse et al., 2007; Andreev et al., 2009) confirm Allerød (PZ IIa of Oy7-11) and Younger Dryas (PZ IIb of Oy7-11) ages of the Late Glacial pollen records. Warmer conditions (MTWA: 8-12 °C) than today have already been reconstructed for the Allerød and the early Holocene, using pollen records from Bol'shoy Lyakhovsky Island (Andreev et al., 2009).

The ostracod records point to stable aquatic conditions during the last period of the Late Glacial. The highest numbers and rich assemblages of ostracod remains were found in such sediments. Obviously, thermokarst development started some time before the Holocene.

The uppermost sequence accumulated under subaerial conditions in a boggy polygonal tundra environment. Ice wedges syngenetic to the boggy deposits are present. Their stable isotope record clearly differs from those of Glacial ice wedges of post-Eemian age, pointing to warmer conditions during the Holocene. Numerous peat inclusions or single peat layers were found in a sandy silt matrix with ice bands and a lens-like cryostructure between single bands which indicate simultaneous (syngenetic) freezing of the sediments at the time of accumulation. An early Holocene shrubby tundra vegetation is reconstructed from the pollen spectra, whereas the pollen spectra indicate late Holocene cooling and a shift to modern tundra vegetation. The ostracod assemblages from the early Holocene are sparse and generally low diverse. As in the Eemian record, the prevailing species are tolerant to changes in the temperature and salinity regimes. The up-filling (aggradation) of the Late Glacial lake environment and its successive transformation into polygonal tundra may be deduced from the ostracod record. Moreover, the preservation of ostracod calcite in an organic-rich milieu such as the boggy horizon is generally poor (Wetterich et al., 2005). Therefore, ostracods

likely occurred in Holocene polygonal ponds, but were not preserved due to acidic conditions in peaty deposits.

5.3 Palaeoenvironmental interpretation of ostracod calcite $\delta^{18}O$ data

The stable oxygen isotope ($\delta^{18}O$) data from ostracod calcite reflect the stable isotope composition of the host water (at the time of shell formation) which itself mostly depends on temperature regime and evaporation effects (e.g. Wetterich et al., 2008a, b). The stable isotope composition of thermokarst lakes in the permafrost zone is mostly influenced by precipitation waters and, to a lesser degree, by the melt water from the surrounding and underlying permafrost. Available $\delta^{18}O$ annual precipitation data from Central Yakutia (Station Yakutsk: 1997 to 2006) average about −23.1‰ and from North Yakutia (Station Tiksi: 2003 to 2007) about −24.4‰ (Kloss, 2008). These values are fairly similar considering the latitudal distance of about 1500 km between them. Assuming a similar precipitation input, the lake water $\delta^{18}O$ is also influenced by local temperature and resulting evaporation effects which are stronger in Central Yakutia due to higher temperatures (Wetterich et al., 2008a). Consequently, the $\delta^{18}O$ in lake waters is controlled by the climatic setting. The $\delta^{18}O$ ostracod calcite data reflect the lake water composition and can therefore be assumed to indicate the water temperature and evaporation regime of lakes.

Comparing the fossil data to the very scarce modern reference data of ostracod $\delta^{18}O$ and water temperatures where those ostracods are found, some preliminary conclusions for the palaeo-temperature regime of waters can be drawn. As shown in Figure 16, heavier stable $\delta^{18}O$ values are obtained from specimens of the Eemian and Late Glacial ostracod *Candona candida* than from the same modern species found today, suggesting conditions of warmer mean water temperatures and/or higher evaporation during the ancient as compared to the modern North Yakutia. Furthermore, when a second modern data set from continental Central Yakutia is compared with the fossil $\delta^{18}O$ records, the fossil records are lighter; this can likely

be interpreted as colder and/or lower evaporation conditions for the ancient as compared to the modern Central Yakutia. The rare water temperature data from the North Yakutian site for the months of June and July (relevant for ostracod growth) show averages of T_{June} = 8.4 °C and T_{July} = 11.1 °C (measured in 2007/08, 0.24 m below the water surface; unpublished data from Samoylov Island, Lena Delta; kindly provided by Julia Boike, SPARC group, AWI Potsdam). Distinctly warmer conditions were documented in continental Central Yakutian thermokarst lakes where T_{June} = 19.1 °C and T_{July} = 19.2 °C (measured in 2005, 0.4 m below the water surface; Wetterich et al., 2008a).

Considering the sparse database, a quantitative palaeo-temperature estimation is actually impossible since continuous temperature data are rare and ostracod monitoring in northern regions and accompanying stable isotope analyses are still lacking. However, because the fossil $\delta^{18}O$ values from the Eemian and also from the Late Glacial clearly fall between modern reference $\delta^{18}O$ values of about −15‰ and −10‰ (reflecting mean summer water temperatures of about 10 °C and 19 °C, respectively), an approximate palaeo-temperature range can be assumed for the palaeo-lakes during both periods. Such fairly accurate estimation is also supported by the above mentioned MTWA temperature reconstruction of 7.8 to 9.6 °C (by pollen data) and ≈12.5°C (by plant macrofossil data) for the Eemian thermal optimum, and 8-12 °C (by pollen data) for the Late Glacial/Holocene period.

6 Conclusions

The studied permafrost exposures on the northern and southern coasts of the Dmitry Laptev Strait contain warm-stage Eemian Interglacial and Holocene deposits as well as underlying deposits reflecting the glacial-interglacial transitions. The multi-proxy palaeoenvironmental record from both periods constructed using sedimentological, cryolithological, and palaeontological methods indicates a general pattern of landscape development according to changes in the climatic setting. The transition from glacial to interglacial conditions is

accompanied by extensive thawing of permafrost (thermokarst), which leads to the formation of basins, or so-called thermokarst depressions. Thawing ice wedges of the former glacial period are transformed into ice wedge pseudomorphs and preserve well-bedded deposits of the thermokarst lakes developing above. Underlying deposits transform into taberal deposits due to thawing. Lacustrine sequences above the taberal horizons contain rich palaeontological records. Further climate change leading to colder and drier conditions in the case of the Eemian/Early Weichselian boundary results in disappearing thermokarst lakes and the development of a polygonal tundra landscape which is reflected in thick sequences of late Pleistocene Ice Complex. In the case of the Late Glacial/Holocene boundary, lakes which had already formed during the Late Glacial warming period at ≈12 kyr BP (Allerød) underwent succession stages and were transformed into boggy polygonal tundra with considerable peat accumulation. Evidence of the three landscape development stages, including (1) thermokarst-induced formation of basins, (2) accumulation of lacustrine sequences, and (3) transformation of lake-dominated areas into polygonal tundra, was obtained and studied for both time slices, and these stages are therefore considered to be of stratigraphical significance (Figure 17).

The Eemian record presented here is to be one of the northernmost terrestrial records in existence from the last Interglacial. Abundant *Larix* pollen have been found in Middle Eemian deposits from Oyogos Yar, but are absent from the northerly Middle Eemian records from Bol'shoy Lyakhovsky Island (Andreev et al., 2004; Ilyashuk et al., 2006), likely indicating that the northern tree line was located near the Oyogos Yar region during the Eemian thermal optimum. The Late Glacial/Holocene records correlate very well with data from the Laptev Sea coastal lowland concerning the onset of permafrost degradation during the Allerød and the general vegetation dynamics (Grosse et al., 2007; Andreev et al., 2009).

In the course of ostracod studies depositional records like those described above can be used for taxonomical and geochemical studies. The Eemian associations contain more taxa than the Late Glacial/Holocene. However, apart from three species (*C.* cf. *neglecta, L.*

suessenbornensis, L. laevis) in the Eemian and one species (*T. glacialis*) in the Late Glacial/Holocene sequences the ostracod associations are similar. Comparable habitats in thermokarst lakes are therefore assumed for both periods. Increasing occurrence of ostracods in lacustrine deposits could be correlated with the Eemian thermal optimum and the Allerød warm period. Only six of the species presented here also occurred in the Late Weichselian association studied at Bykovsky Peninsula and in the Lena River Delta (Wetterich et al., 2005, 2008c). This first presentation of interglacial freshwater ostracod associations from Arctic periglacial environments can be used as a reference for understanding similar Quaternary periglacial records in Europe.

The application of ostracods as a palaeo-proxy in permafrost sediments by comparing ancient data to modern reference data is a relative new approach to understanding palaeo-archive permafrost; expanding the modern database of species ecology, the modern geochemical reference data of host waters, and the database of stable isotope data from ostracod calcite would improve the accuracy of this method. However, initial assumptions that can be made from comparing Eemian and Late Glacial fossil ostracods to modern reference assemblages were presented here. The $\delta^{18}O$ data from the fossil ostracods indicate an approximate mean summer water temperature range between 10 and 19 °C in the palaeo-lakes during both periods. Future monitoring of modern associations in thermokarst lakes and polygonal ponds in connection with continuous climate and hydrological observations will expand the database and improve our ability to utilize ostracods as a palaeoenvironmental indicator.

Acknowledgements

The study presented is part of the Russian–German cooperative scientific effort, “System Laptev Sea” and the International Polar Year project “Past Permafrost” (IPY project 15). Pollen analyses and radiocarbon dating were funded by the German Science Foundation (DFG) within the framework of the project “Late Quaternary warm phases in the Arctic”

(DFG SCHI 975/1). We thank all Russian and German colleagues who helped us during fieldwork in 2007 (Tatyana Kuznetsova, Vladimir Tumskoy, Dmitry Dobrynin, Aleksandr Derevyagin from Moscow State University; Thomas Opel from AWI Potsdam; Frank Kienast from Senckenberg Institute Weimar). The analytical work in the laboratories at the Alfred Wegener Institute Potsdam was greatly supported by Ute Bastian, Judith Walter, Ulrike Hoff and Lutz Schönicke. Ilona Schäpan and Helga Kemnitz (Deutsches GeoForschungsZentrum Potsdam, Germany) helped with SEM photography of ostracod valves. The paper really benefited by valuable comments and English language correction from Candace O'Connor (University of Alaska, Fairbanks).

References

Alm, G., 1914. Beiträge zur Kenntnis der nördlichen und arktischen Ostracodenfauna. Arkiv för Zoologi 9, 1-20 (in German).

Andreev, A.A., Grosse, G., Schirrmeister, L., Kuzmina, S.A., Novenko, E.Y., Bobrov, A.A., Tarasov, P.E., Kuznetsova, T.V., Krbetschek, M., Meyer, H., Kunitsky, V.V., 2004. Late Saalian and Eemian palaeoenvironmental history of the Bol'shoy Lyakhovsky Island (Laptev Sea region, Arctic Siberia). Boreas 33, 319-348.

Andreev, A.A., Grosse, G., Schirrmeister, L., Kuznetsova, T.V., Kuzmina, S.A., Bobrov, A.A., Tarasov, P.E., Novenko, E.Y., Meyer, H., Derevyagin, A.Y. and co-authors, 2009. Weichselian and Holocene palaeoenvironmental history of the Bol'shoy Lyakhovsky Island, New Siberian Archipelago, Arctic Siberia. Boreas 38, 72-110.

Arkhangelov, A.A., Mikhalev, D.V., Nikolaev, V.I., 1996. Rekonstruktsiya uslovii formirovaniya mnogoletnei merzloty i paleoklimatov Severnoi Evrazii (Reconstruction of

formation conditions of permafrost and palaeoclimate of northern Eurasia). In: Velichko, A.A., Arkhangelov, A.A., Borisova, O.K., Gribchenko, Y.N., Drenova, A.N., Zelikson, E.M., Kurenkova, E.N., Mikhalev, D.V., Nikolaev, V.I., Novenko, E.Y. and co-editors (Eds.), Razvitie oblasti mnnogoletnei merzloty i periglyatsial'noi zony Severnoi Evrazii i usloviya rasseleniya drevnego cheloveka (History of permafrost regions and periglacial zones of Northern Eurasia and conditions of old human settlement). Russian Academy of Science, Institute of Geography, Moscow, pp. 85-109 (in Russian).

Berglund, B.E., Ralska-Jasiewiczowa, M., 1986. Pollen analysis and pollen diagrams. In: Berglund, B. (Ed.), Handbook of Holocene Palaeoecology and Palaeohydrology. Interscience, New York, pp. 455-484.

Bunge, A.A., 1887. Bericht über den ferneren Gang der Expedition. Reise nach den Neusibirischen Inseln. Aufenthalt auf der Grossen Ljachof-Insel. In: Schrenk, L.V., Maximovicz, C.J. (Eds.), Expedition zu den Neusibirischen Inseln und dem Jana-Lande (1885). Beiträge zur Kenntnis des russischen Reiches und der angrenzenden Länder Vol. III. Kaiserliche Akademie der Wissenschaften, St. Petersburg, pp. 231-284 (in German).

Chersky, I.D., 1891. Opisanie kollektsiy posletretichnykh iskopaemykh zhivotnykh, sobrannykh Novo-Sibirskoi ekspeditsiei 1885-1886 gg (The description of the collection of post-Tertiary animals, collected by the New Siberian expedition in 1885-1886). Zapiski Imperatorskoi Akademii Nauk (Notes of the Russian Imperial Academy of Science) 65, 1-707 (in Russian).

Craig, H., 1961. Isotopic variations in meteoric waters. Science 133, 1702-1703.

Diebel, K., 1968. Neue *Limnocythere*-Arten (Ostracoda) aus dem deutschen Pleistozän. Monatsberichte der Deutschen Akademie der Wissenschaften zu Berlin 10, 519-538 (in German).

Diebel, K., Pietrzeniuk, E., 1969. Ostracoden aus dem Mittelpleistozän von Süßenborn bei Weimar. Paläontologische Abhandlungen A III, 463-488 (in German).

French, H.M., 2007. The periglacial environment. 3rd edition. Wiley, Chichester, 458 pp.

Gravis, G.F., 1978. Cyclicity of thermokarst at the coastal lowlands during the late Pleistocene and Holocene. In: Publications of the 3rd International Permafrost Conference. July 10-13, 1978, Edmonton, Alberta, Canada Vol. 1, pp. 283-287.

Grimm, E., 1991. Tilia and Tiliagraph. Illinois State Museum, Springfield, Illinois, USA.

Grimm, E., 2004. Tilia, Tilia·Graph and TGView 2.0.2. Illinois State Museum, Springfield, USA.

Grosse, G., Schirrmeister, L., Siegert, C., Kunitsky, V.V., Slagoda, E.A., Andreev, A.A., Dereviagin, A.Y., 2007. Geological and geomorphological evolution of a sedimentary periglacial landscape in Northeast Siberia during the Late Quaternary. Geomorphology 86, 25-51.

Hammarlund, D., Edwards, T.W.D., Björk, S., Buchardt, B., Wohlfahrt, B., 1999. Climate and environment during the Younger Dryas (GS-1) as reflected by composite stable isotope

records of lacustrine carbonates at Torreberga, southern Sweden. Journal of Quaternary Science 14, 17-28.

Igarashi, Y., Fukuda, M., Nagaoka, D., Saljo, K., 1995. Vegetation and climate during accumulating period of Yedoma, inferred from pollen records. In: Takahashi, K., Osawa, A., Kanazawa, Y. (Eds.), Proceedings of the third symposium on the joint Siberian permafrost studies between Japan and Russia in 1994. Hokkaido University Press, Sapporo, pp. 139-146.

Ilyashuk, B.P., Andreev, A.A., Bobrov, A.A., Tumskoy, V.E., Ilyashuk, E.A., 2006. Interglacial history of a palaeo-lake and regional environment: A multi-proxy study of a permafrost deposit from Bol'shoi Lyakhovsky Island, Arctic Siberia. Journal of Paleolimnology 36, 855-872.

Ivanov, O.A., 1972. Stratigrafiya i korrelatsiya Neogenykh i Chetvertichnykh otlozheniyakh subarkticheskikh ravnin Vostochnoi Yakutii (Stratigraphy and correlation of Neogene and Quaternary deposits of subarctic plains in Eastern Yakutia). In: Problemy izucheniya Chetvertichnogo perioda (Problems of the Quaternary studies). Nauka, Moscow, pp. 202-211 (in Russian).

Kaplina, T.N., Giterman, R.E., Lakhtina, O.V., Abrashov, B.A., Kiselyov, S.V., Sher, A.V., 1978. Duvannyi Yar – opornyi razrez pozdnepleistotsenovykh oltozhenii Kolymskoi nizmenosti (Duvannyi Yar – a key section of Upper Pleistocene deposits of the Kolyma lowland). Byulleten' komissii po izucheniyu chetvertichnogo perioda (Bulletin of the Commission on Quaternary Research) 48, 49-65 (in Russian).

Kaplina, T.N., Sher, A.V., Giterman, R.E., Zazhigin, V.S., Kiselyov, S.V., Lozhkin, A.V., Nikitin, V.P., 1980. Opornyi razrez pleistotsenovykh otlozhenii na reke Allaikha - nizov'ya Indigirki (Key section of Pleistocene deposits on the Allaikha River - lower reaches of the Indigirka). Byulleten' komissii po izucheniyu chetvertichnogo perioda (Bulletin of the Commission on Quaternary Research) 50, 73-95 (in Russian).

Kayalainen, V.I., Kulakov, Y.N., 1966. K voprosy paleogeografii Yana-Indigirskoi nizmenosti v Neogeno-Chetvertichnom periode (To the questions of Paleogeography of the Yana-Indigirka coastal lowland during the Neogene-Quaternary period). In: Saks, V.N. (Ed.), Chetvertichnyi period v Sibiri (Quaternary period of Siberia). Nauka, Moscow, pp. 274-283 (in Russian).

Keatings, K.W., Heaton, T.H.E., Holmes, J.A., 2002. Carbon and oxygen fractionation in non-marine ostracods: Results from a 'natural culture' environment. Geochimica et Cosmochimica Acta 66, 1701-1711.

Keatings, K.W., Holmes, J.A., Heaton, T.H.E., 2006. Effects of pre-treatment on ostracod valve chemistry. Chemical Geology 235, 250-261.

Kienast, F., Tarasov, P., Schirrmeister, L., Grosse, G., Andreev, A.A., 2008. Continental climate in the East Siberian Arctic during the last interglacial: implications from palaeobotanical records. Global and Planetary Change 60, 535-562.

Kloss, A.L., 2008. Water isotope geochemistry of recent precipitation in Central and North Siberia as a proxy for the local and regional climate system. Unpublished diploma thesis,

Institute for Physical Geography and Landscape Ecology, Leibniz University of Hannover, Germany, 107 pp.

Konishchev, V.N., Kolesnikov, S.F., 1981. Osobennosti stroeniya i sostava pozdnekainozoiskikh otlozheniyakh v obnazhenii Oyagosskii Yar (Specifics of structure and composition of late Cenozoic deposits in the section of Oyogossky Yar). In: Problemy Kriolitologii (Problems of Cryolithology) Vol. IX, Moscow State University Publishers, Moscow, pp. 107-117 (in Russian).

Kunitsky, V.V., 1996. Khimicheskii sostav ledinykh zhil ledovogo kompleksa (Chemical content of ice wedges of the Ice complex). In: Razvitie kriolitozony v Evrazii v verkhnem Kenozoe (Development of the Cryolithozone of Eurasia during the upper Cenozoic). Russian Academy of Science, Siberian branch, Permafrost Institute Yakutsk, pp. 93-117 (in Russian).

Kunitsky, V.V., 1998. Ledovyi kompleks i krioplanatsionnye terrasy ostrova Bol'shogo Lyakhovskogo (Ice Complex and cryoplanation terraces of the Bol'shoy Lyakhovsky Island) In: Kamensky, R.M., Kunitsky, V.V., Olovin, B.A., Shepelev, V.V. (Eds.), Problemy Geokriologii (Problems of Geocryology). Russian Academy of Science, Siberian branch, Permafrost Institute Yakutsk, pp. 60-72 (in Russian).

Kunitsky, V.V., Grigoriev, M.N., 2000. Boulders and cobble roundstones near the Svyatoy Nos Cape and on Big Lyakhovsky Island. In: Abstracts of the 4th QUEEN Workshop, Lund, Sweden, April 7-10, 2000. pp. 62.

Lozhkin, A.V., Anderson, P.M., 1995. The Last Interglaciation in Northeast Siberia. Quaternary Research 43, 147-158.

Lozkhin, A.V., Anderson, P.M., Matrosova, T.V., Minyuk, P., 2007. The pollen record from El'gygytgyn Lake: implications for vegetation and climate histories of northern Chukotka since the late middle Pleistocene. Journal of Paleolimnology 37, 135-153.

Meisch, C., 2000. Freshwater Ostracoda of Western and Central Europe. Spektrum Akademischer Verlag, Heidelberg, Berlin, 522 pp.

Meyer, H., Schönicke, L., Wand, U., Hubberten, H.-W., Friedrichsen, H., 2000. Isotope studies of hydrogen and oxygen in ground ice - Experiences with the equilibration technique. Isotopes in Environmental and Health Studies 36, 133-149.

Meyer, H., Dereviagin, A.Y., Siegert, C., Schirrmeister, L., Hubberten, H.-W., 2002. Paleoclimate reconstruction on Big Lyakhovsky Island, North Siberia - Hydrogen and oxygen isotopes in ice wedges. Permafrost and Periglacial Processes 13, 91-105.

Nadeau, M.J., Schleicher, M., Grootes, P.M., Erlenkeuser, H., Gottdang, A., Mous, D.J.W., Sarnthein, J.M., Willkomm, H., 1997. The Leibniz-Labor facility at the Christian-Albrecht-University, Kiel, Germany. Nuclear Instruments and Methods in Physics Research 123, 22-30.

Nadeau, M.J., Grootes, P.M., Schleicher, M., Hasselberg, P., Rieck, A., Bitterling, M., 1998. Sample throughput and data quality at the Leibniz-Labor AMS facility. Radiocarbon 40, 239-245.

Nagaoka, D., Saijo, K., Fukuda, M., 1995. Sedimental environment of the Yedoma in high Arctic eastern Siberia. In: Proceedings of the third symposium on the joint Siberian permafrost studies between Japan and Russia in 1994. Hokkaido University Press, Sapporo, pp. 8-13.

Nikolsky, P.A., Basilyan, A.E., 2004. Mys Svyatoi Nos - Opornyi razrez chetvertichnykh otlozhenii severa Yana-Indigiskoi nizmenosti (Mys Svyatoi Nos - a Quaternary key section of the northern Yana-Indigirka lowland). In: Estestvenaya istoriya rossiskoi vostochnoi Arktiki v Pleistotsene i Golotsene (Natural history of the Russian Eastern Arctic during the Pleistocene and Holocene). GEOS, Moscow, pp. 5-13 (in Russian).

Opel, T., Derevyagin, A.Yu., Meyer, H., Schirrmeister, L., Wetterich S., submitted. Paleoclimatic information from stable water isotopes of Holocene ice wedges at the Dmitrii Laptev Strait (Northeast Siberia). Permafrost and Periglacial Processes, Special Issue in 2009 "Isotope and Geochemical characteristics of permafrost".

Pietrzeniuk, E., 1977. Ostracoden aus Thermokarstseen und Altwässern in Zentral-Jakutien. Mitteilungen des Zoologischen Museums zu Berlin 53, 331-362 (in German).

Pirumova, L.G., 1968. Diatomovye vodorosli v chetvertichnykh otlozheniyakh Yana-Indigiskoi nizmenosti i Bol'shogo Lyakhovskogo ostrova (Diatoms in Quaternary sediments of northern Yana-Indigirka lowland and Bol'shoy Lyakhovsky Island). In: Zhuze, A.P. (Ed.), Iskopaemye diatomovye vodorosli SSSR (Fossil diatoms of the USSR). Nauka, Moscow, pp. 80-83 (in Russian).

Reimer, P.J., Baillie, M.G.L., Bard, E., Bayliss, A., Beck, J.W., Bertrand, C., Blackwell, P.G., Buck, C.E., Burr, G., Cutler, K.B. and co-authors, 2004. INTCAL04 terrestrial radiocarbon age calibration, 0-26 cal kyr BP. Radiocarbon 46, 1029-1058.

Rivas-Martínez, S., 2007 Global Bioclimatics. Data set. Phytosociological Research Center, Madrid, Spain (published online: http://www.globalbioclimatics.org).

Romanovskii, N.N., 1958a. Novye dannye o stroenii chetvertichnykh otlozhenii ostrova Bol'shogo Lyakhovskogo, Novosibirskie ostrova (New data about Quaternary deposits structure on the Bol'shoy Lyakhovsky Island, New Siberian Islands). Nauchnye doklady vysshei shkoly. Seriya geologogeograficheskaya (Scientific notes of the higher school. Geological-geographical series) 2, 243-248 (in Russian).

Romanovskii, N.N., 1958b. Paleogeograficheskie usloviya obrazovaniya chetvertichnykh otlozhenii ostrova Bol'shogo Lyakhovskogo, Novosibirskie ostrova (Paleogeographical conditions of formation of the Quaternary deposits on the Bol'shoy Lyakhovsky Island, New Siberian Islands). Voprosy fizicheskoi geografii polyarnykh stran (Questions of Physical Geography in Polar regions) Vol. I, pp. 80-88 (in Russian).

Romanovskii, N.N., 1958c. Merzlotnye structury oblekaniya v chetvertichnykh otlozheniyakh (Permafrost structures in Quaternary deposits). Nauchnye doklady vysshei shkoly. Seriya geologo-geograficheskaya (Scientific notes of the higher school. Geological-geographical series) 3, 185-189 (in Russian).

Romanovskii, N.N., Gavrilov, A.V., Tumskoy, V.E., Kholodov, A.L,, Siegert, C., Hubberten, H.-W., Sher, A.V., 2000. Environmental evolution in the Laptev Sea region during Late Pleistocene and Holocene. Polarforschung 68, 237-245.

Romanovskii, N.N., Hubberten, H.-W., 2001. Results of Permafrost Modelling of the Lowlands and Shelf of the Laptev Sea Region, Russia. Permafrost and Periglacial Processes 12, 191-202.

Schirrmeister, L., Oezen, D., Geyh, M.A., 2002a. ^{230}Th/U Dating of Frozen peat, Bol'shoy Lyakhovsky Island (Northern Siberia). Quaternary Research 57, 253-258.

Schirrmeister, L., Siegert, C., Kunitsky, V.V., Grootes, P.M. Erlenkeuser, H., 2002b. Late Quaternary ice-rich Permafrost sequences as a paleoenvironmental archive for the Laptev Sea Region in northern Siberia. International Journal of Earth Sciences 91, 154-167.

Schirrmeister, L., Siegert, C., Kuznetsova, T., Kuzmina, S., Andreev, A.A., Kienast, F., Meyer, H., Bobrov, A.A., 2002c. Paleoenvironmental and paleoclimatic records from permafrost deposits in the Arctic region of Northern Siberia. Quaternary International 89, 97-118.

Schirrmeister, L., Grosse, G., Schwamborn, G., Andreev, A.A., Meyer, H., Kunitsky, V.V., Kuznetsova, T.V., Dorozhkina, M.V., Pavlova, E.Y., Bobrov, A.A., Oezen, D., 2003. Late Quaternary history of the accumulation plain north of the Chekanovsky Ridge (Lena Delta, Russia): a multidisciplinary approach. Polar Geography 27, 277-319.

Schirrmeister, L., Grosse, G., Kunitsky, V., Magens, D., Meyer, H., Dereviagin, A., Kuznetsova, T., Andreev,.A., Babiy, O., Kienast, F. and co-authors, 2008. Periglacial landscape evolution and environmental changes of Arctic lowland areas for the last 60 000 years (western Laptev Sea coast, Cape Mamontov Klyk). Polar Research 27, 249-272.

Schirrmeister, L., Wetterich, S., Kunitsky, V., Tumskoy, V., Dobrynin, D., Derevyagyn, A., Opel, T., Kienast, F., Kuznetsova, T., Gorodinsky, A., 2009. Palaeoenviromental studies on the Oyogos Yar coast. In: Boike, J., Bol'shiyanov, D.Y., Schirrmeister, L., Wetterich, S. (Eds.), The Expedition LENA - NEW SIBERIAN ISLANDS 2007 during the International Polar Year (IPY) 2007/2008. Berichte zur Polar- und Meeresforschung 584, 85-154.

Sher, A.V., Kuzmina, S.A., Kuznetsova, T.V., Sulerzhinsky, L.D., 2005. New insights into the Weichselian environment and climate of the East Siberian Arctic, derived from fossil insects, plants, and mammals. Quaternary Science Reviews 24, 533-569.

Sirocko, F., Claussen, M., Sánchez Goñi, F.M., Litt, T. (Eds.) 2007. The Climate of Past Interglacials. Developments in Quaternary Science 7, Elsevier, Amsterdam, 622 pp.

Stuiver, M., Polach, H.A., 1977. Discussion: Reporting of ^{14}C data. Radiocarbon 19, 355-363.

Symon, L., Arris, L. and Heal, B. (Eds.), 2005. Arctic Climate Impact Assessment (ACIA). Cambridge University Press, Cambridge and New York, 1042 pp. (published online: http://www.acia.uaf.edu).

Tarasov, P., Granoszweski, W., Bezrukova, E., Brewer, S., Nita, M., Abzaeva, A., Oberhänsli, H., 2005. Quantitative reconstruction of the last interglacial vegetation and climate based on pollen record from Lake Baikal, Russia. Climate Dynamics 25, 625-637.

Tumskoy, V.E., Basilyan, A.E., 2006. Opornyi razrez chetvertichnykh otlozhenii ostrova Bol'shoy Lyakhovsky (Key section of Quaternary deposits on Bol'shoy Lyakhovsky Island) In: Problemy korrelatsii pleistotsenovykh sobytii na Russkom Severe COPERN (Correlation problems of Pleistocene Events in the Russian North). COPERN abstracts. December 4-6, 2006, St. Petersburg, pp. 106-107 (in Russian).

van Everdingen, R. (Ed.), 1998, revised May 2005. Multi-language glossary of permafrost and related ground-ice terms. Boulder, CO: National Snow and Ice Data Center/World Data Center for Glaciology (published online: http://nsidc.org/fgdc/glossary/).

Velichko, A.A., Curry, B., Ehlers, J., 2005. Main Quaternary chronostratigraphical units used in Siberia, East-European Plain, West Europe and North America. In: Velichko, A.A., Nechaev, V.P. (Eds.), Cenozoic climatic and environmental changes in Russia. The Geological Society of America Special Paper 382: pp. XVII.

Velichko, A.A., Nechaev, V.P. (Eds.), 2005. Cenozoic Climatic and Environmental Changes in Russia. Geological Society of America Special Paper 382, 226 pp.

Vereshchagin, V.N. (Ed.), 1982. Stratigraficheskii slovar' SSSR. Paleogen, Neogen i Chetvertichnaya sistema (Stratigraphical dictionary of the USSR. Palaeogene, Neogene, Quaternary system). Nauka, Moscow, 128 pp. (in Russian).

von Grafenstein, U., Erlenkeuser, H., Trimborn, P., 1999. Oxygen and carbon isotopes in modern fresh-water ostracod valves: Assessing vital offsets and autecological effects of interest for palaeoclimate studies. Palaeogeography Palaeoclimatology Palaeoecology 148, 133-152.

von Toll, E.V., 1897. Iskopaemye ledniki Novo-Sibirskikh ostrovov, ikh otnoshenie k trupam mamontov i k lednikovomu periodu (Ancient glaciers of New Siberian Islands, their relation to mammoth corpses and the Glacial period). Zapiski Imperatorskogo Russkogo Geograficheskogo obshestva po obshei geografii (Notes of the Russian Imperial Geographical Society) 32, 1-137 (in Russian).

Wetterich, S., Schirrmeister, L., Pietrzeniuk, E., 2005. Freshwater ostracodes in Quaternary permafrost deposits in the Siberian Arctic. Journal of Paleolimnology 34, 363-374.

Wetterich, S., Herzschuh, U., Meyer, H., Pestryakova, L., Plessen, B., Lopez, C.M.L., Schirrmeister, L., 2008a. Evaporation effects as reflected in freshwaters and ostracod calcite from modern environments in Central and Northeast Yakutia (East Siberia, Russia). Hydrobiologia 614, 171-195 .

Wetterich, S., Schirrmeister, L., Meyer, H., Viehberg, F.A., Mackensen, A., 2008b. Arctic freshwater ostracods from modern periglacial environment in the Lena River Delta (Siberian Arctic, Russia): geochemical applications for palaeoenvironmental reconstructions. Journal of Paleolimnology 39, 427-449.

Wetterich, S., Kuzmina, S., Andreev, A.A., Kienast, F., Meyer, H., Schirrmeister, L., Kuznetsova, T., Sierralta, M., 2008c. Palaeoenvironmental dynamics inferred from late

Quaternary permafrost deposits on Kurungnakh Island, Lena Delta, Northeast Siberia, Russia. Quaternary Science Reviews 27, 1523-1540.

Figure captions

Figure 1 The coasts of the Dmitry Laptev Strait with exposure positions of the composite Eemian profiles (1) L7-14 and (2) Oy7-08, and the composite Late Glacial/Holocene profiles (3) L7-08, (4) R33 A1 and (5) Oy7-11

Figure 2 Composite Eemian to post-Eemian sequence L7-14 at the south coast of Bol'shoy Lyakhovsky Island (73.28770 °N; 141.69097 °E): (a) Exposure scheme with position of the studied subprofiles A to F; (b) Positions of the sediment samples; (c) Overview picture of the studied sequence; (d) Ice-rich deposits covering the Eemian sequence; (e) Well-bedded Eemian lake deposits in an ice wedge pseudomorph

Figure 3 Comparison of sedimentological, biogeochemical, and cryolithological records of the composite Eemian profiles L7-14 and Oy7-08

Figure 4 Composite Eemian sequence Oy7-08 at the north coast of Oyogos Yar (72.68002 °N; 143.53181 °E): (a) Exposure scheme with positions of the studied subprofiles A and B, sediment samples; (b) Photograph of the positions of subprofiles A and B which occur close together; (c) Detail of the well-bedded sediment structure within the ice wedge cast. For legend see Figure 3

Figure 5 Composite Late Glacial/Holocene thermokarst sequence L7-08 on the south coast of Bol'shoy Lyakhovsky Island (73.28161 °N; 141.83794 °E); (a) Exposure scheme with

positions of the studied subprofiles A to D, sediment samples, and AMS-measured dates (kyr BP); (b) Overview photograph of the studied sequence. For legend see Figure 3

Figure 6 Comparison of sedimentological, biogeochemical, and cryolithological records of the composite Holocene alas profiles and underlying taberal deposits L7-08 and Oy7-11

Figure 7 Composite Late Glacial/Holocene thermokarst sequence Oy7-11 on the north coast of Oyogos Yar (72.68347 °N; 143.47526 °E): (a) Exposure scheme with position of the studied subprofiles A and B, sediment samples, and AMS-measured dates (kyr BP); (b) Overview photograph showing both walls of an erosional crack; (c) Subprofile A with taberal Ice Complex deposits, lacustrine deposits and ice wedge casts, and the covering peat layer. For legend see Figure 3

Figure 8 (a) $\delta^{18}O$–δD plot of post-Eemian Glacial syngenetic ice wedges (Section L7-14) and Holocene syngenetic and epigenetic ice wedges (Section L7-08) with respect to the Global Meteoric Water Line (GMWL), which correlates fresh surface waters on a global scale (Craig 1961); (b) Overview photograph of the sampled Holocene syngenetic ice wedge in the upper part of section L7-08 at 11 m a.s.l.

Figure 9 Eemian pollen record from Bol'shoy Lyakhovsky Island (Section L7-14)

Figure 10 Eemian pollen record from Oyogos Yar (Section Oy7-08)

Figure 11 Late Glacial/Holocene pollen record from Bol'shoy Lyakhovsky Island (Section L7-08)

Figure 12 Late Glacial/Holocene pollen record from Oyogos Yar (Section Oy7-11)

Figure 13 SEM images of fossil ostracod valves (LV - left valve, RV - right valve). *Candona candida*: (1) female LV, (2) female RV; *Fabaeformiscandona harmsworthi*: (3) female LV, (4) female RV; *F. levanderi*: (5) female LV, (6) female RV, (7) male LV, (8) male RV; *F. rawsoni*: (9) female LV, (10) female RV, (11) male LV, (12) male RV; *F. tricicatricosa*: (13) female LV, (14) female RV, (15) male LV, (16) male RV; T. *glacialis*: (17) female LV; *Limnocythere falcata*: (18) female LV, (19) female RV; *Limnocytherina sanctipatricii*: (20) female LV, (21) female RV, (22) male LV, (23) male RV; *Limnocythere suessenbornensis*: (24) female LV, (25) female RV; *Cyclocypris laevis*: (26) female LV, (27) female RV; *Cypria exsculpta*: (28) female LV, (29) female RV; *Ilyocypris lacustris*: (30) female LV, (32) female RV; *Cytherissa lacustris*: (32) female LV, (33) female RV. Note varying 0.5 mm scales for number 1-17 and number 18-33

Figure 14 Ostracod species assemblages from Eemian deposits of Bol'shoy Lyakhovsky Island and Oyogos Yar. Note varying scales

Figure 15 Ostracod species assemblages from Late Glacial/Holocene deposits of Bol'shoy Lyakhovsky Island and Oyogos Yar. Note varying scales

Figure 16 Oxygen and carbon stable isotope signatures (mean values, maxima and minima) of ostracod calcite from different periods. Eemian records are given by light grey symbols, Late Glacial records by dark grey symbols and modern reference records from lakes in North Yakutia (Lena Delta; Wetterich et al. 2008b) and Central Yakutia (Wetterich et al. 2008a) by black symbols. Diamonds indicate data from the species *Candona candida* (and *Candona*

muelleri-jakutica for the modern record from Central Yakutia) and squares indicate data from the species *Cytherissa lacustris*

Figure 17 General scheme of glacial-interglacial landscape dynamics controlled by thermokarst processes

Table captions

Table 1 Synopsis of the stratigraphic units exposed on the Dmitry Laptev Strait. The stratigraphical position of the Bychchagy Suite (grey highlighted) is still unclear

Table 2 AMS-measured radiocarbon ages of plant remains in samples of the Alas sequences from Bol'shoy Lyakhovsky (L7-08) and Oyogos Yar (Oy7-11)

Table 3 Oxygen and hydrogen stable isotope signatures (mean values and standard deviations) of post-Eemian Glacial and Holocene ice wedges (IWs)

Table 4 Taxonomic reference list of all identified ostracod species from Eemian and Late Glacial/Holocene deposits

Table 5 Oxygen and carbon stable isotope signatures (mean values, maxima and minima) of ostracod calcite from different periods

Figure 1

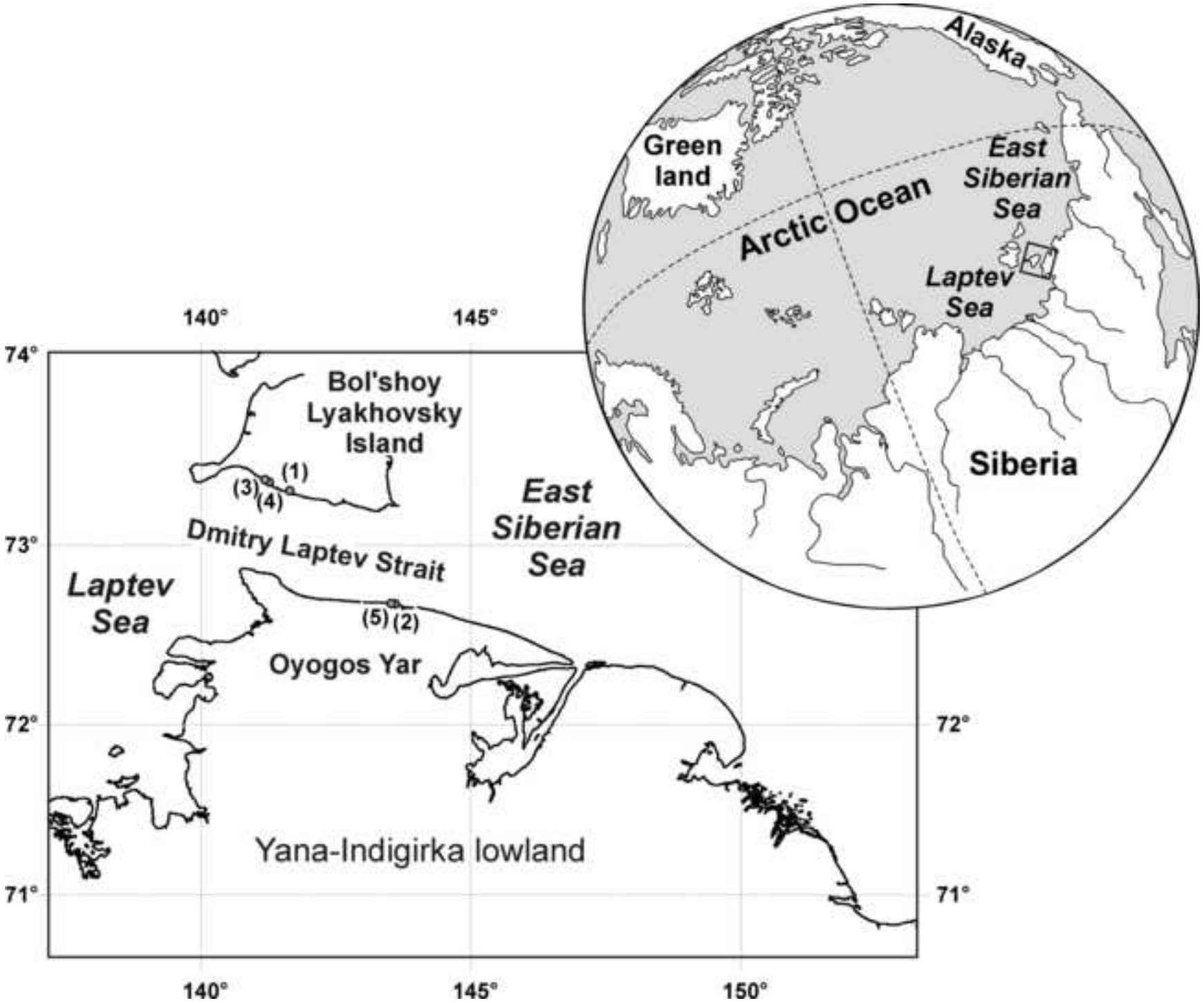

Figure 2

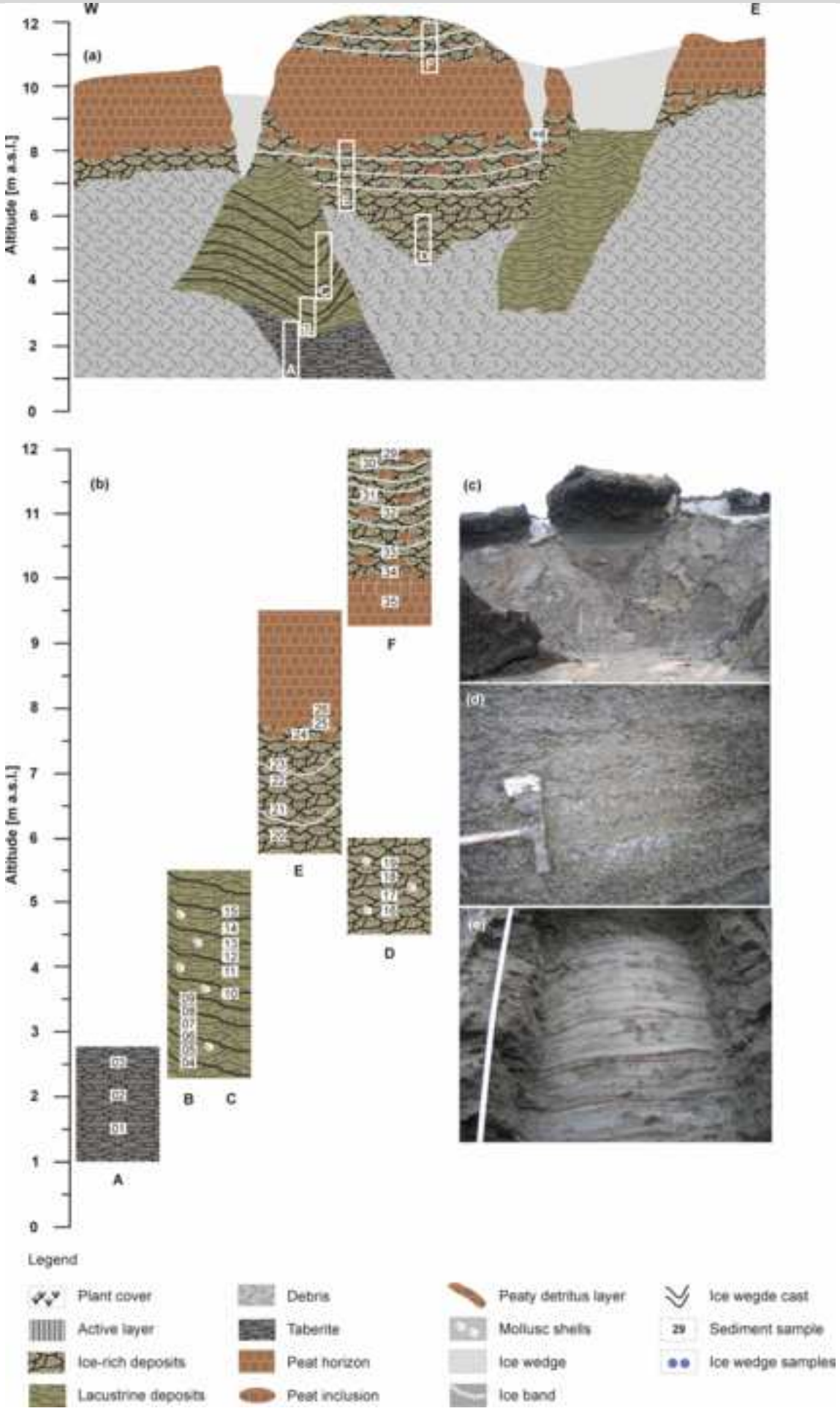

Figure 3

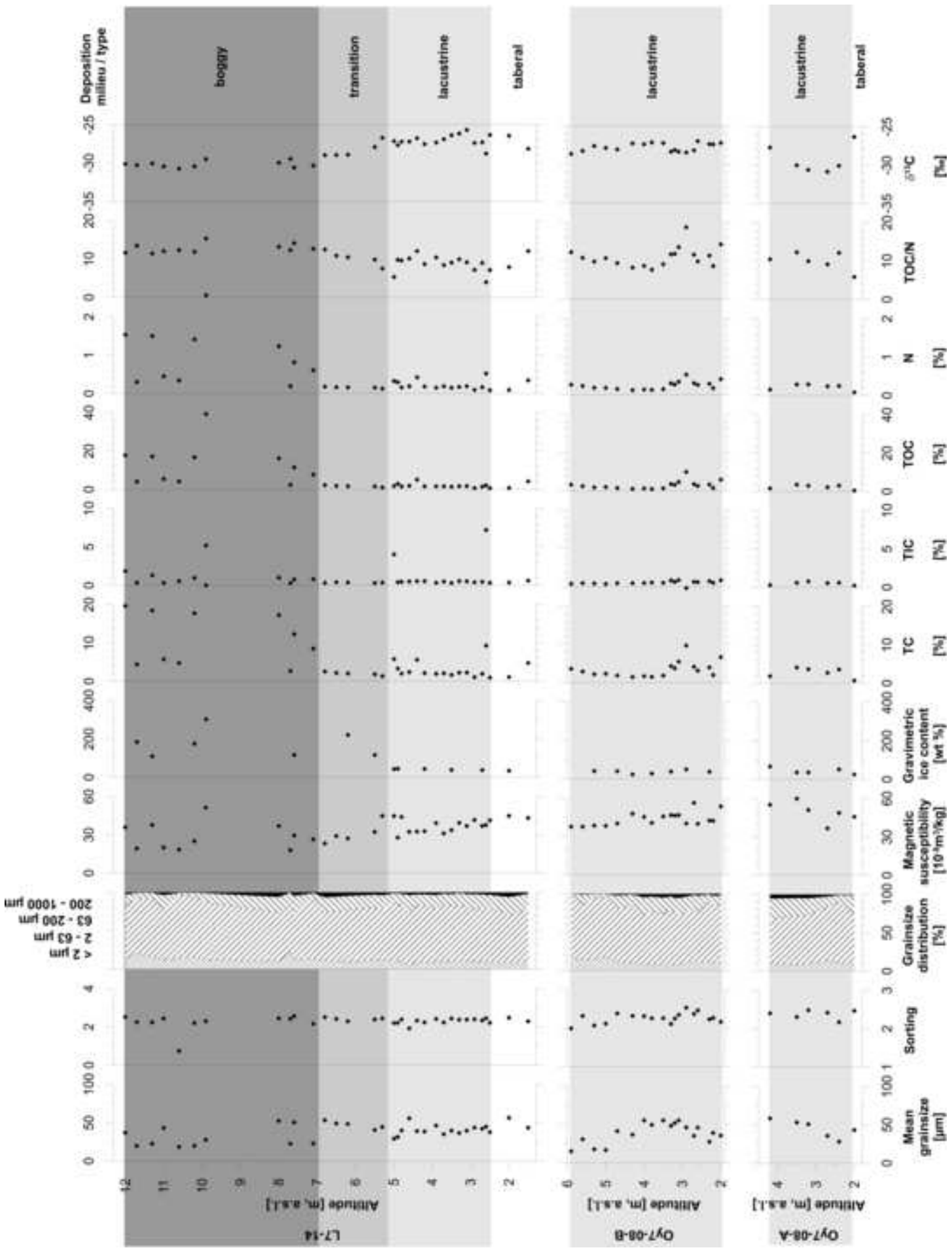

Figure 4

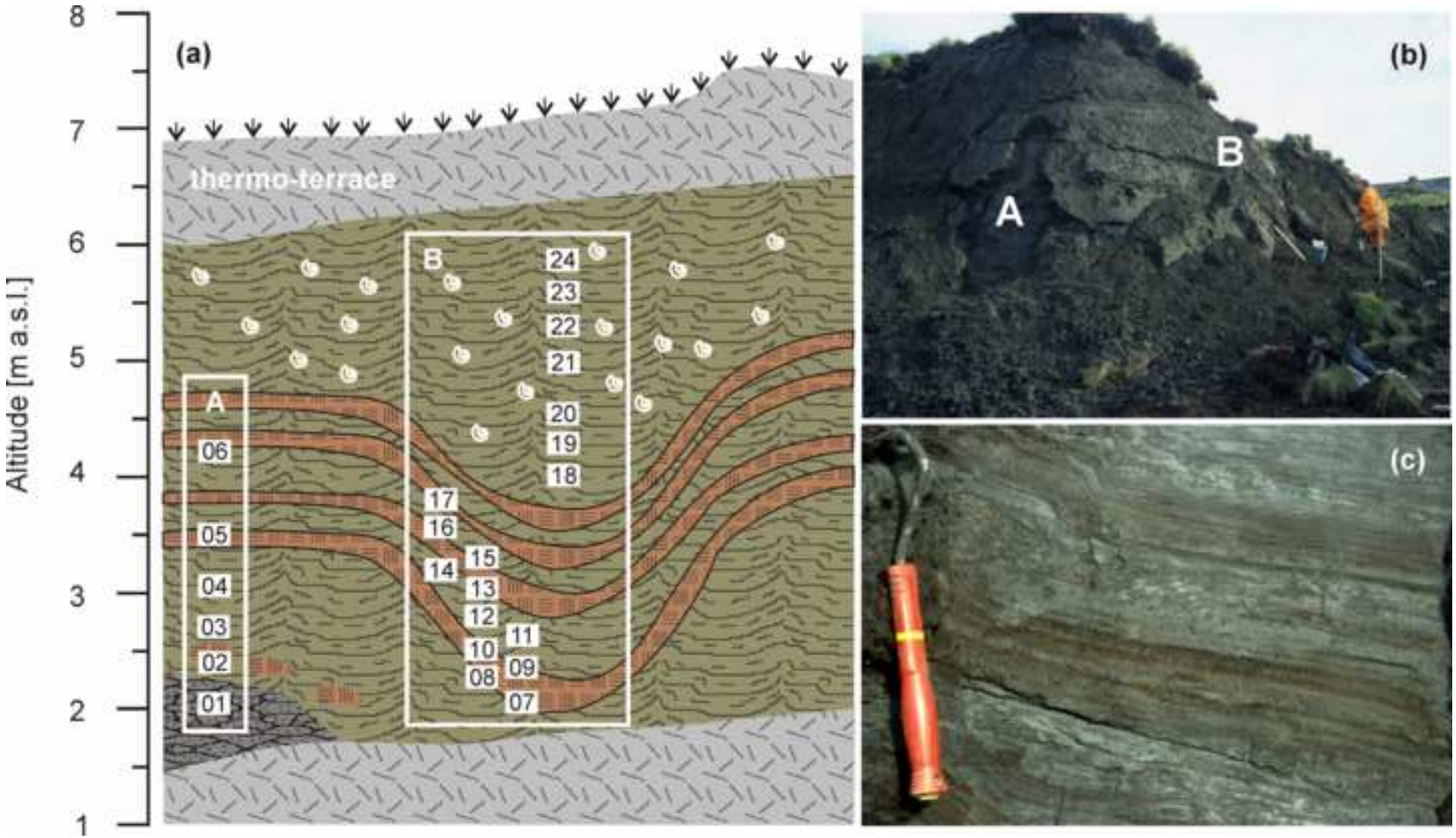

Figure 5

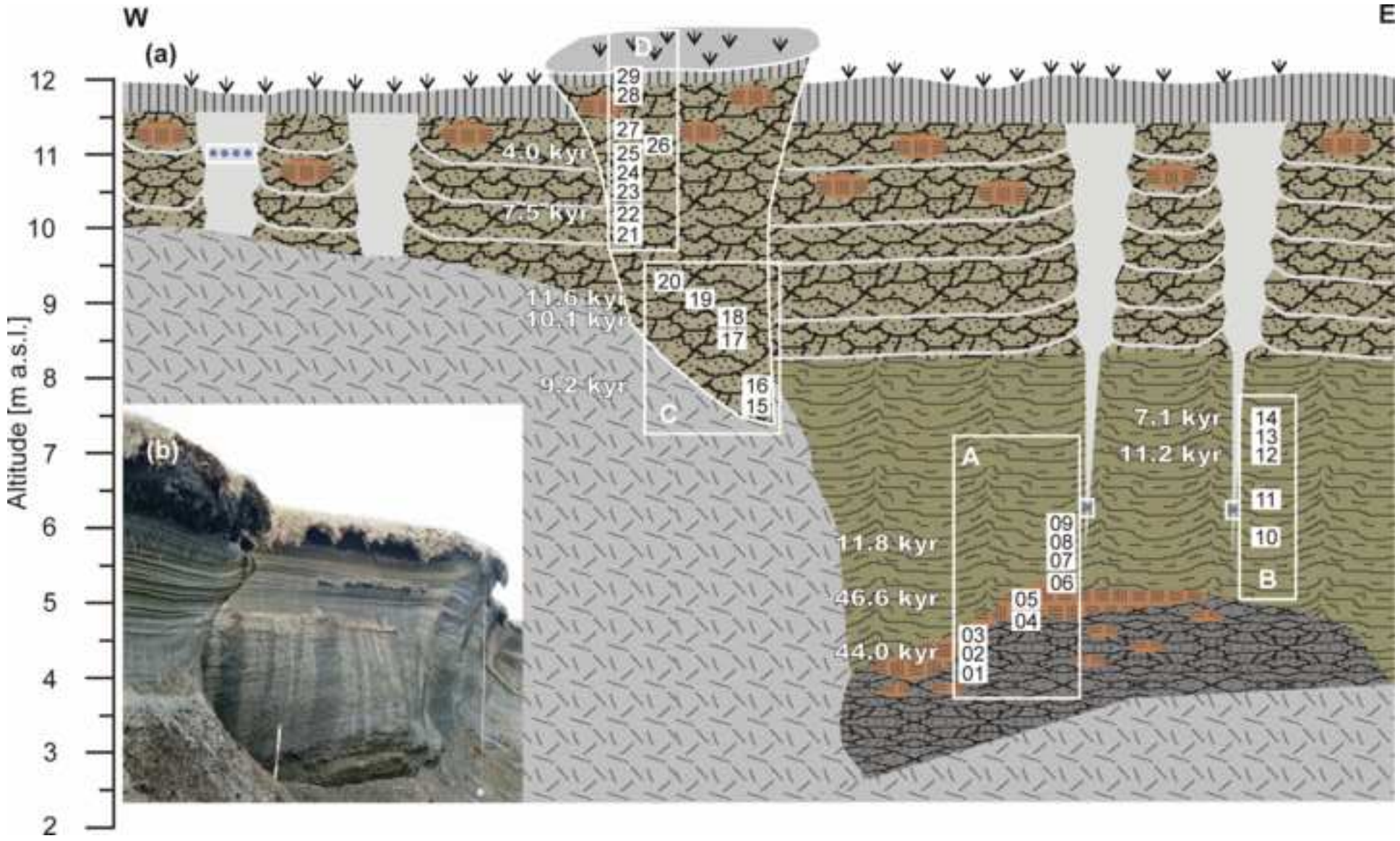

Figure 6

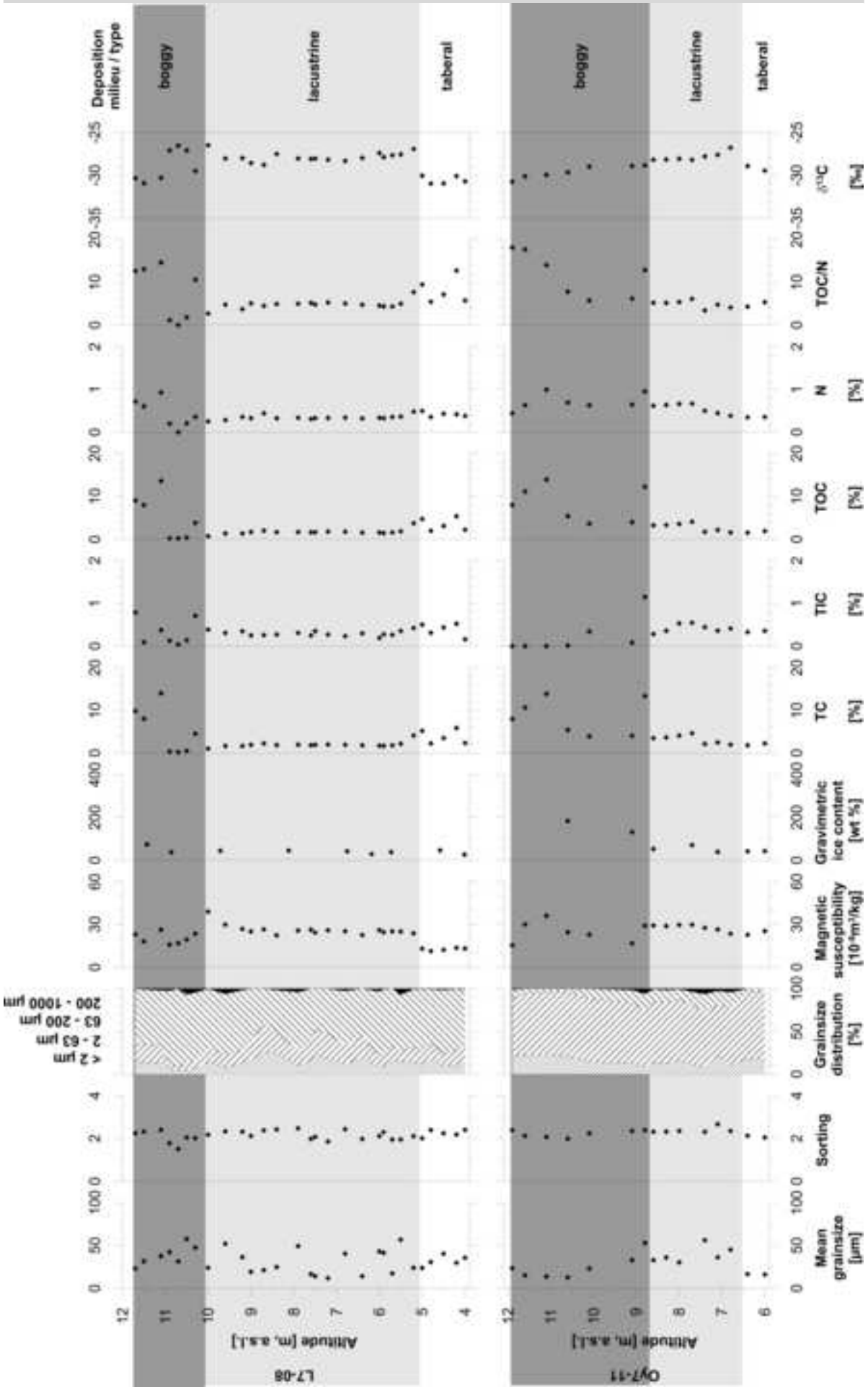

Figure 7

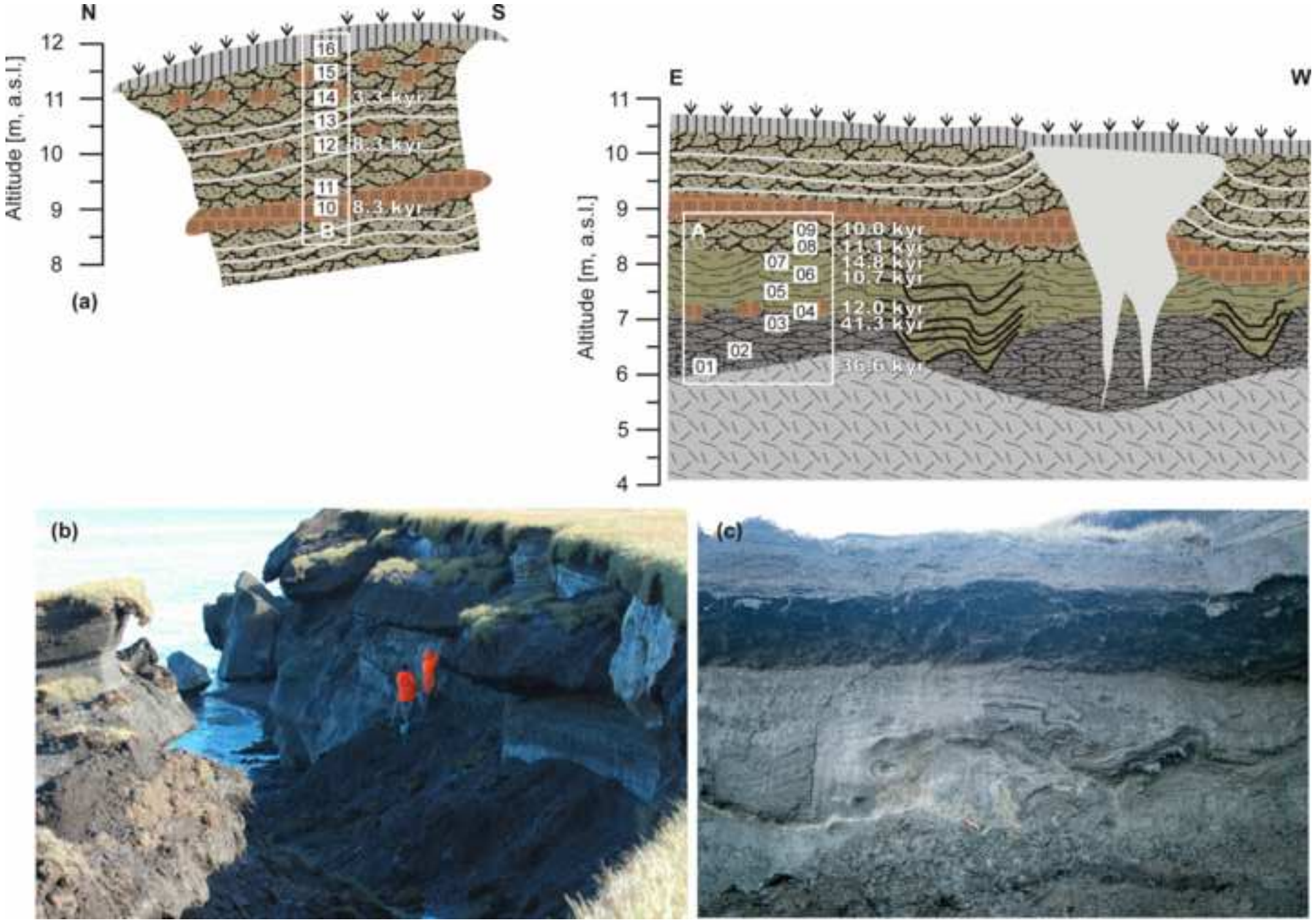

Figure 8

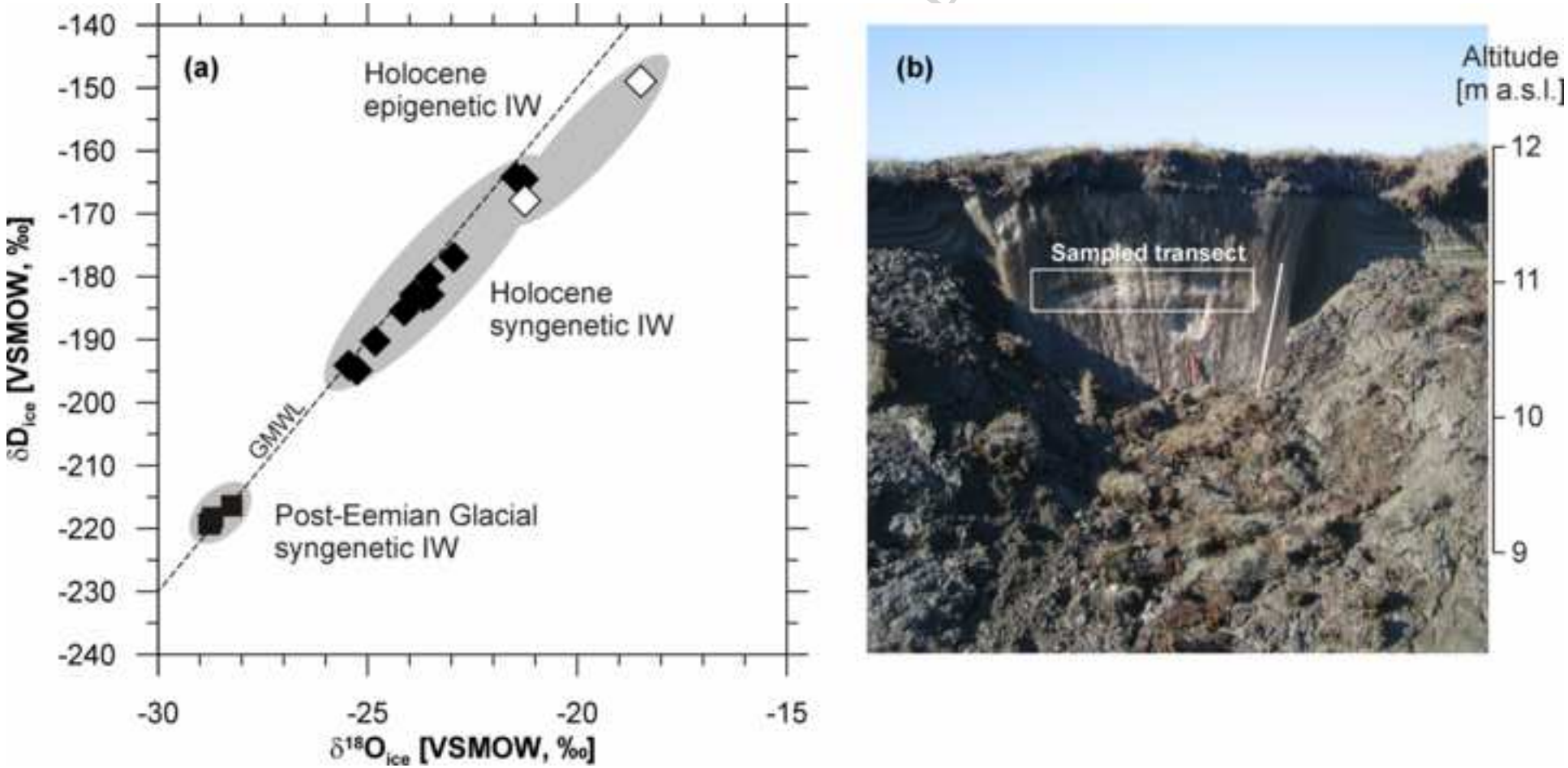

Figure 9

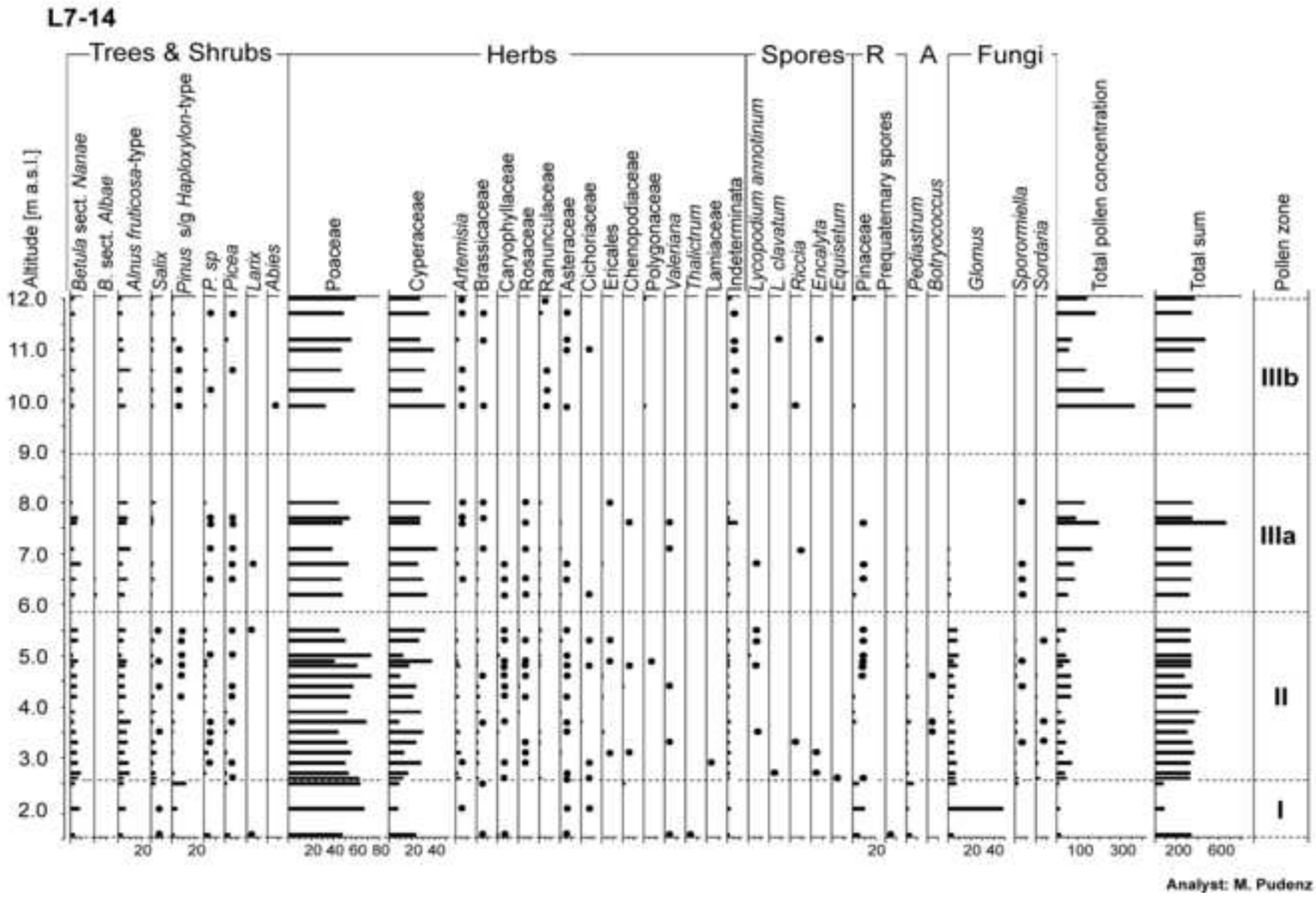

Figure 10

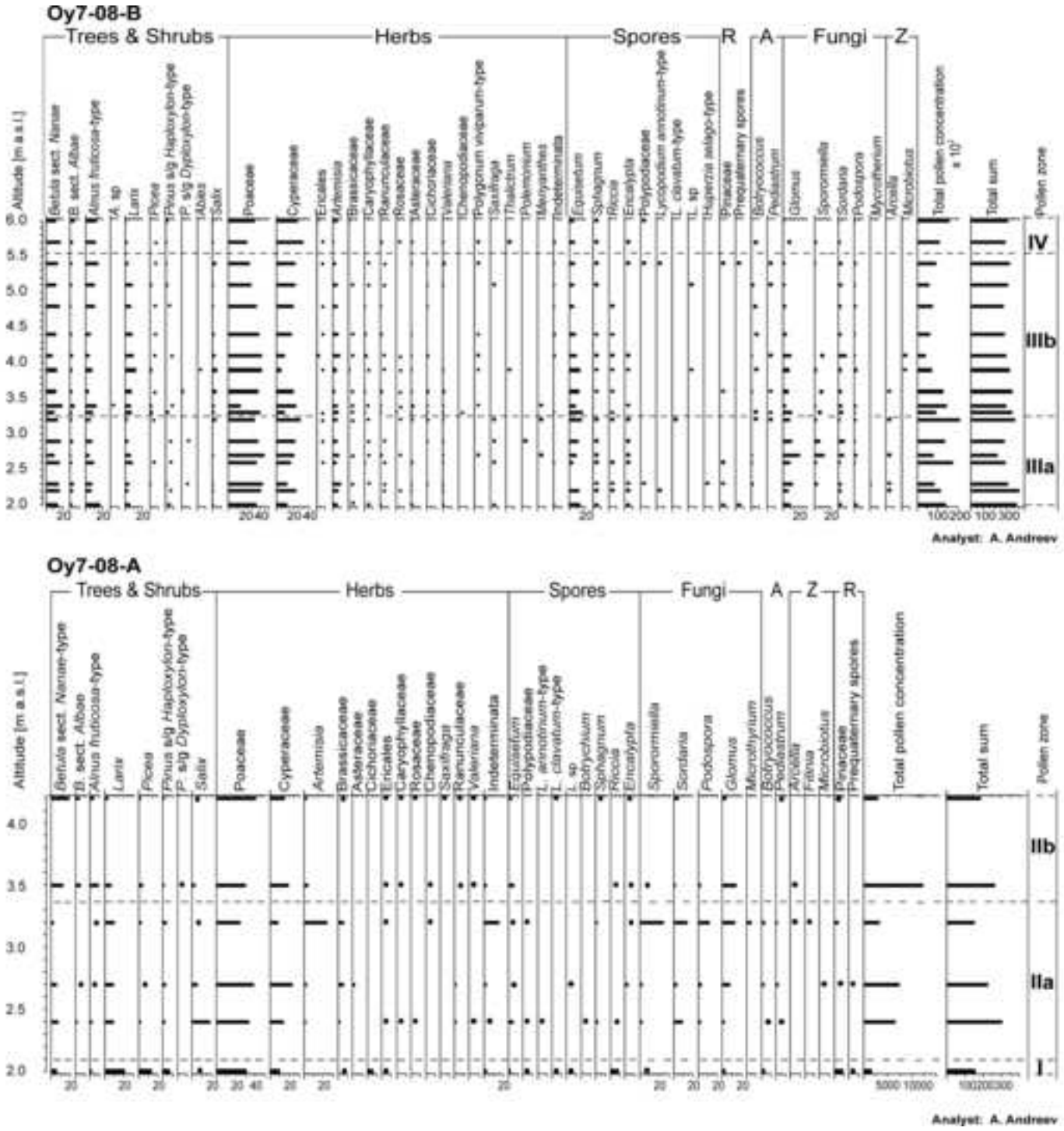

Figure 11

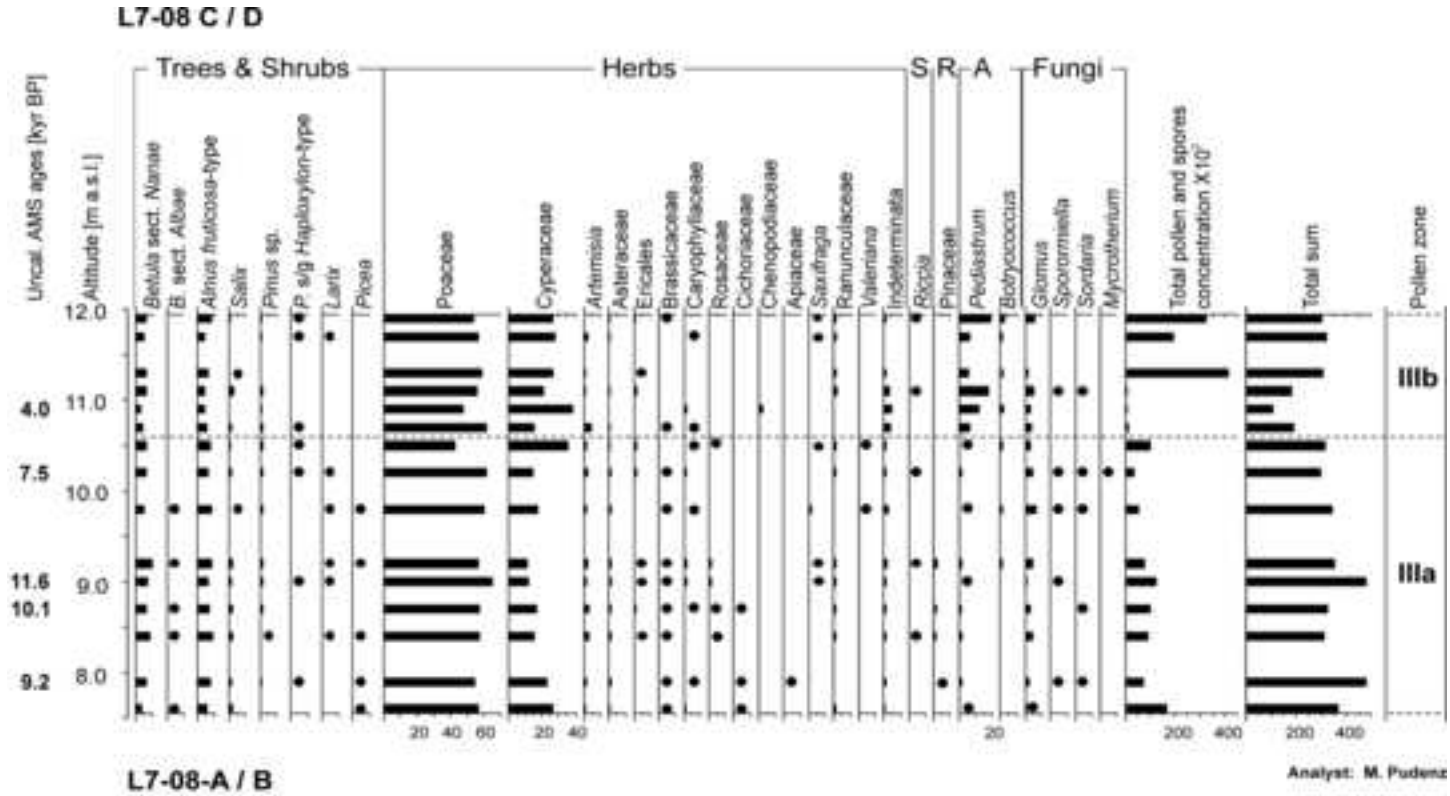

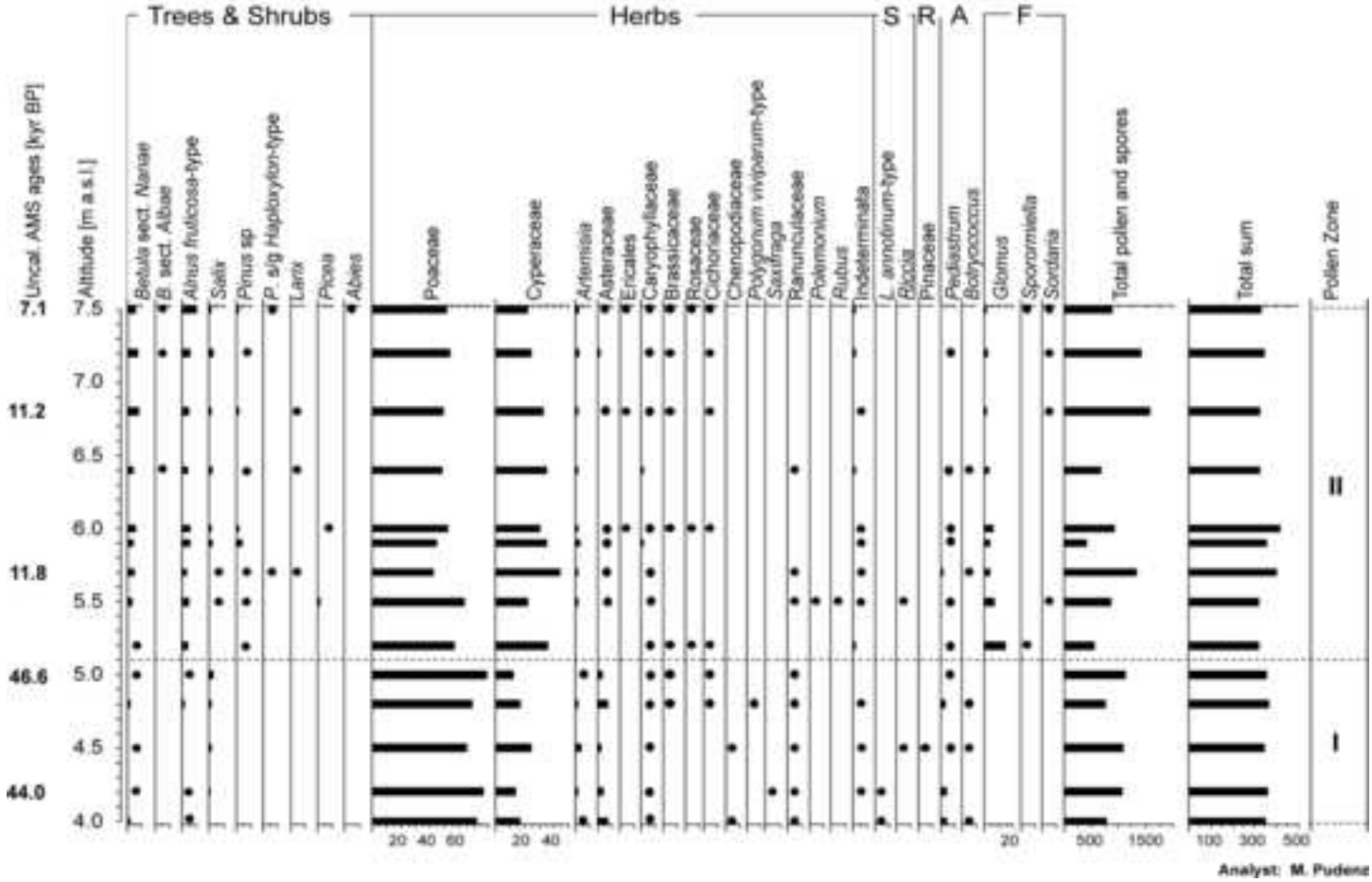

Figure 12

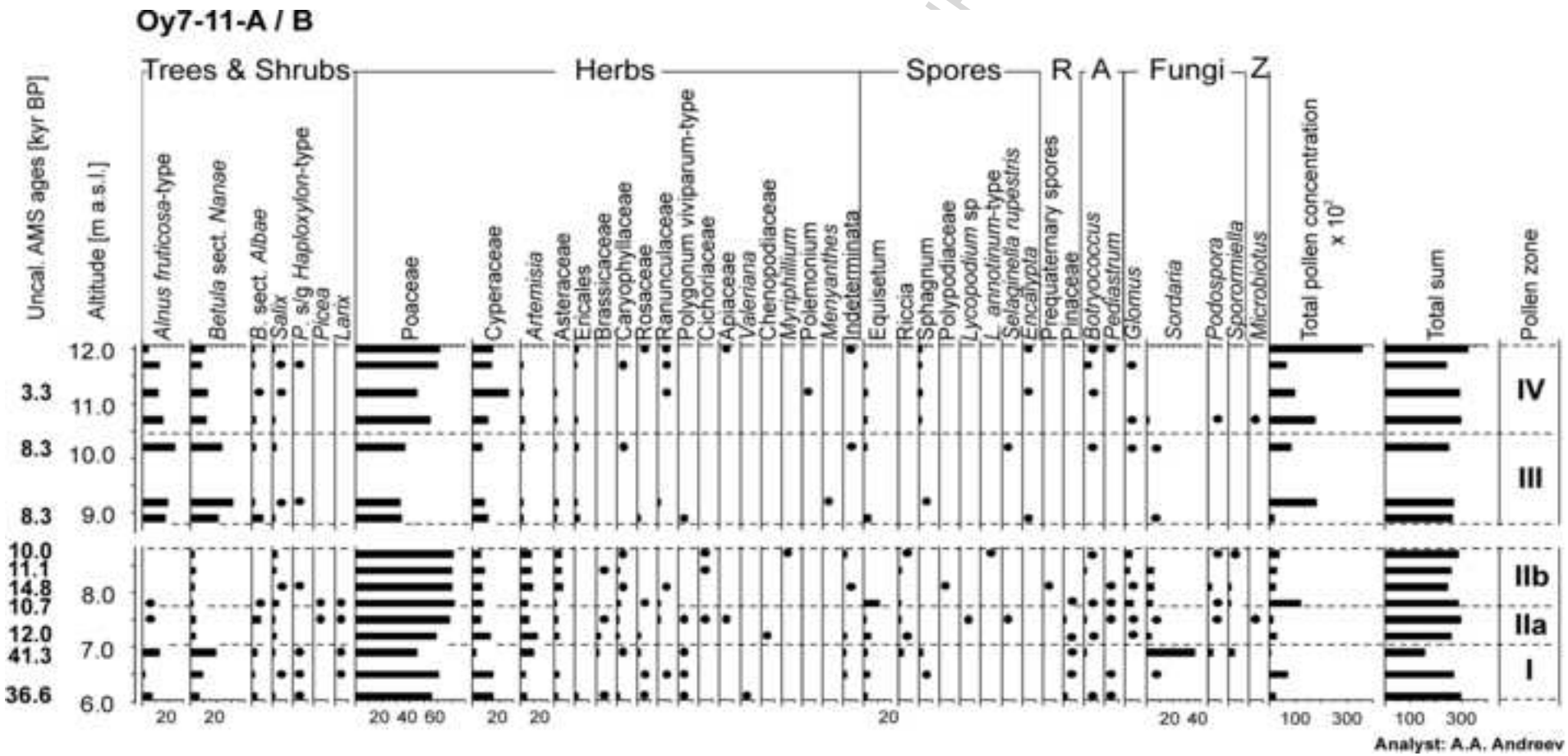

Figure 13

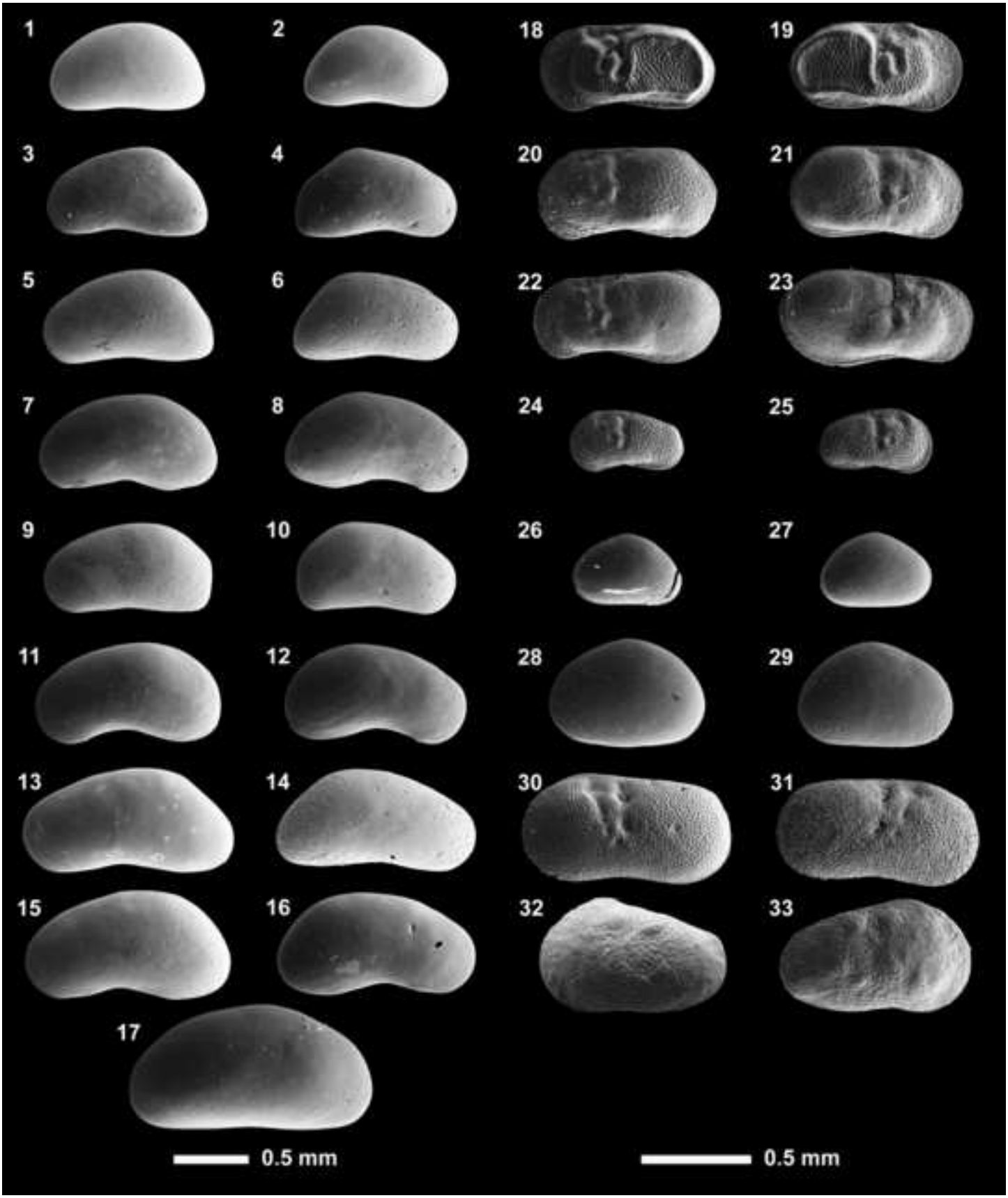

Figure 14

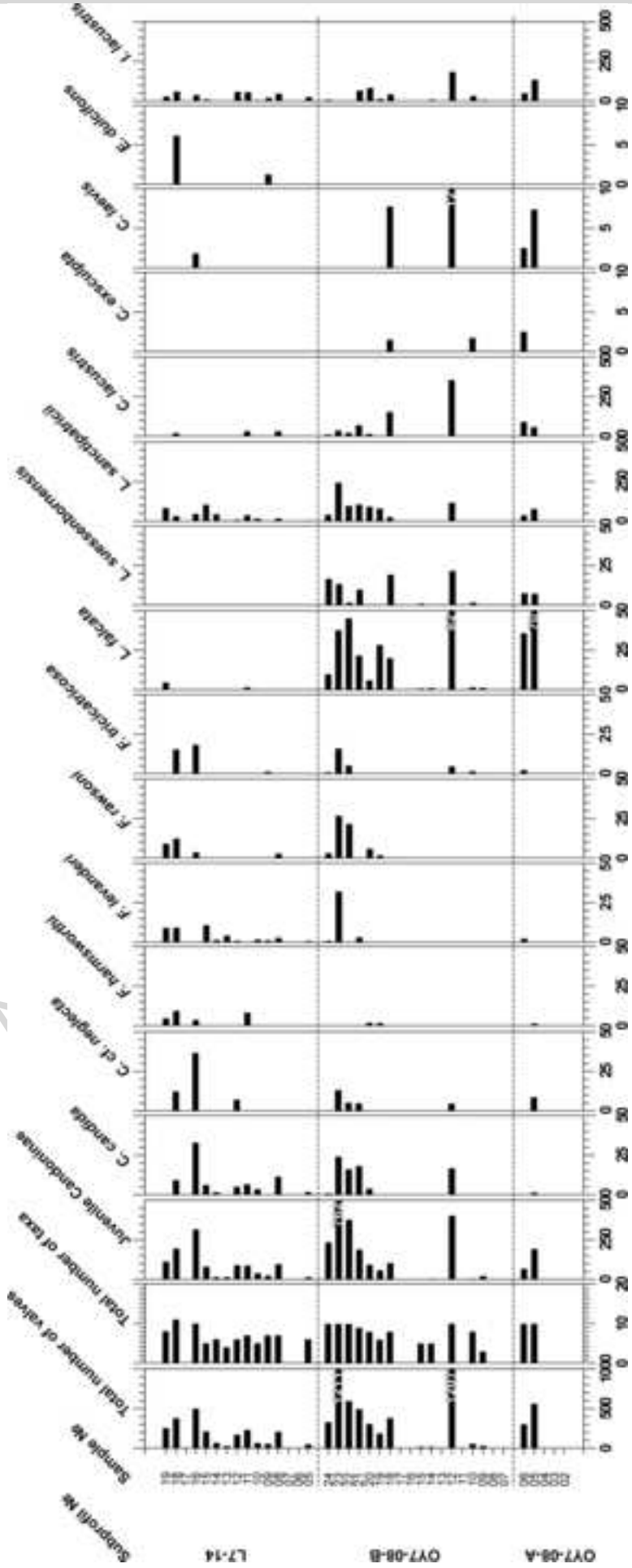

Figure 15

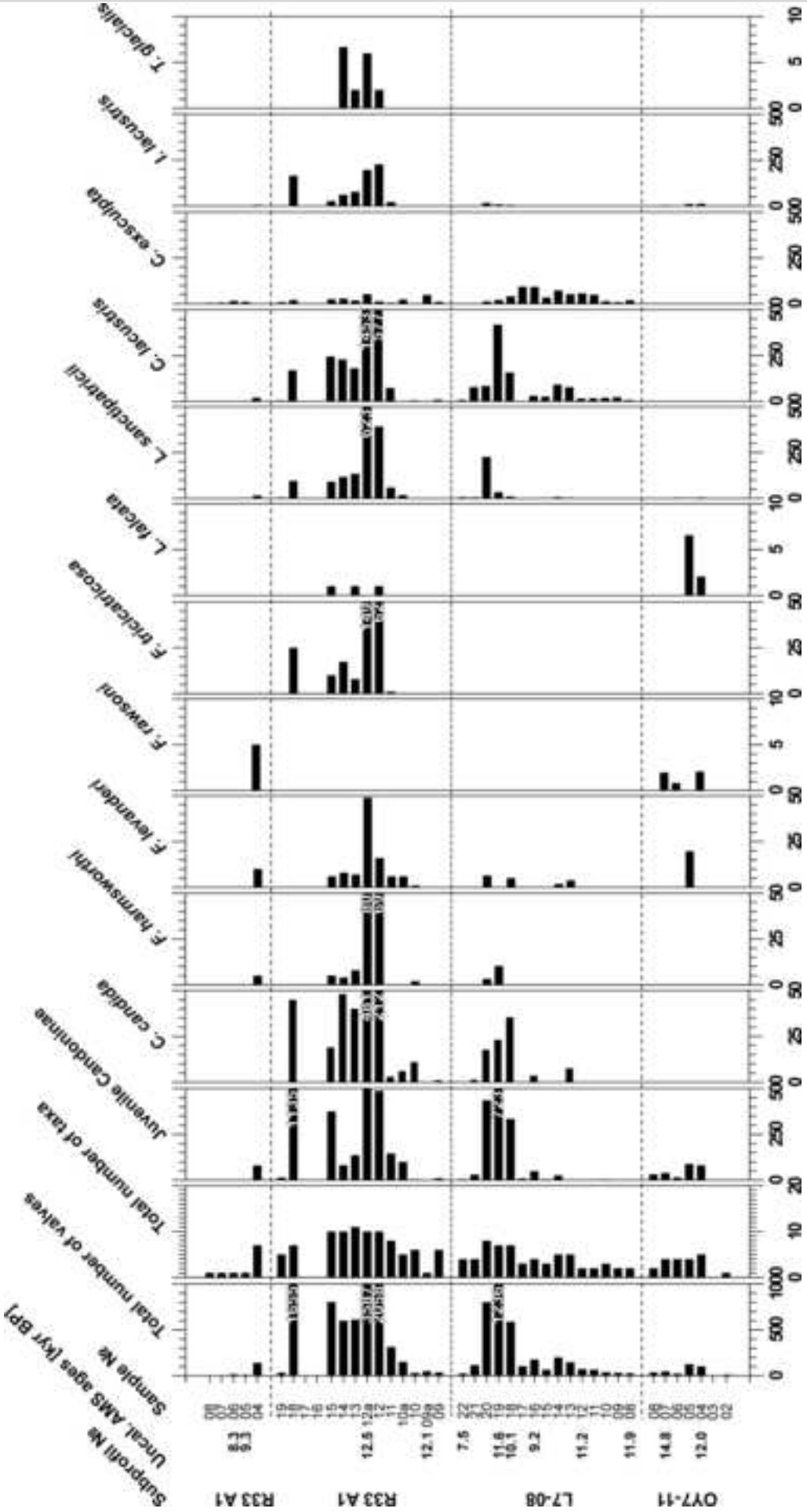

Figure 16

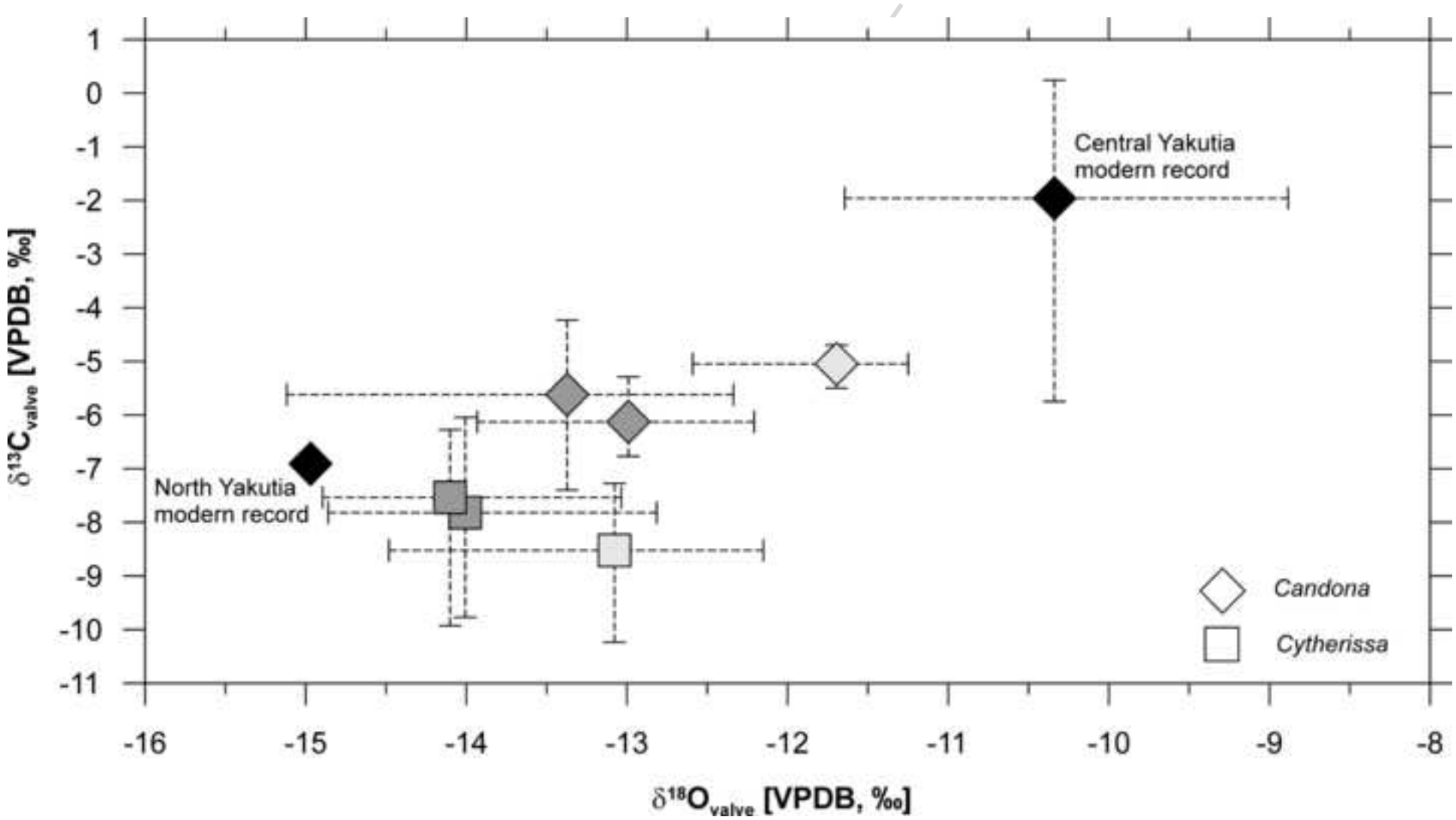

Figure 17

Polygonal tundra of following glacial time or recent period

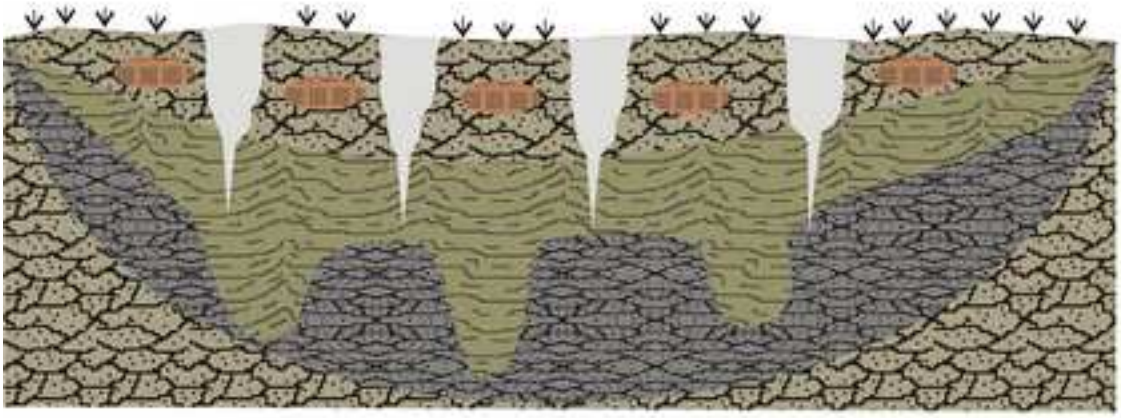

(3) Refreezing below the lake; Filling-up and transition into polygonal tundra

Lake environment of interglacial time

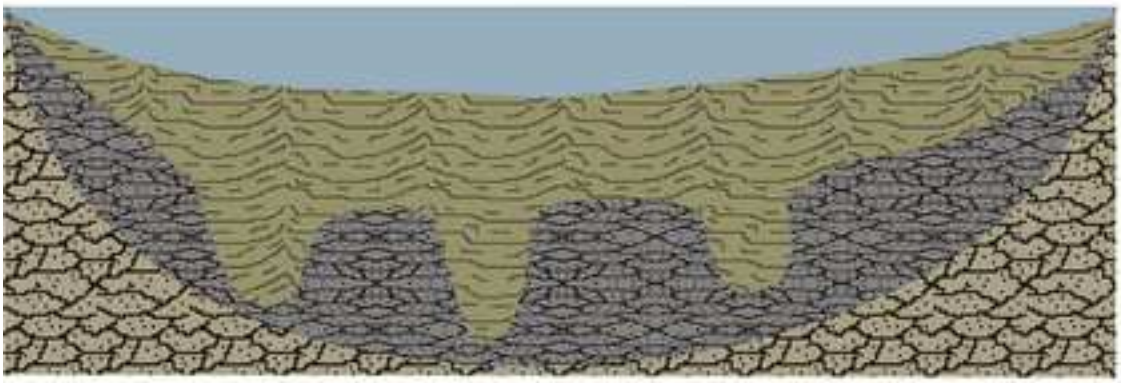

(2) Extensive permafrost melting; Accumulation of laustrine sequences

Lake environment of glacial to interglacial transition

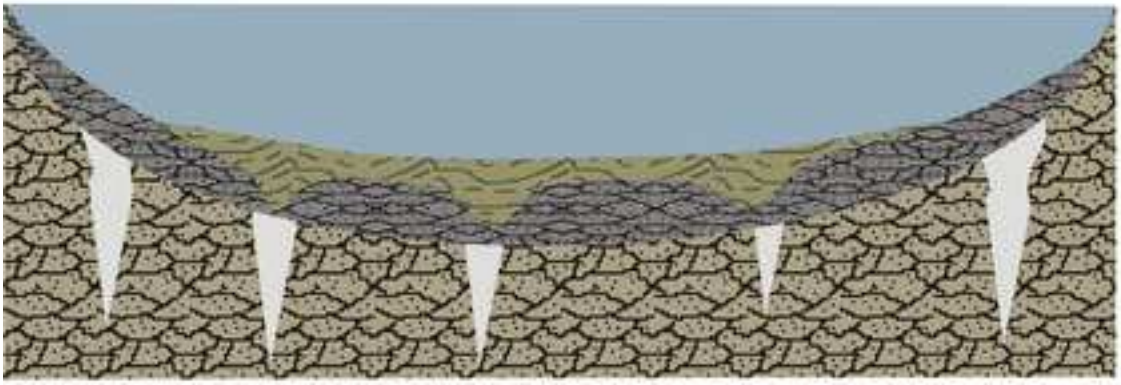

(1) Initial permafrost melting; Formation of thermokarst depressions, ice wedge pseudomorphs and taberites

Polygonal tundra of glacial time

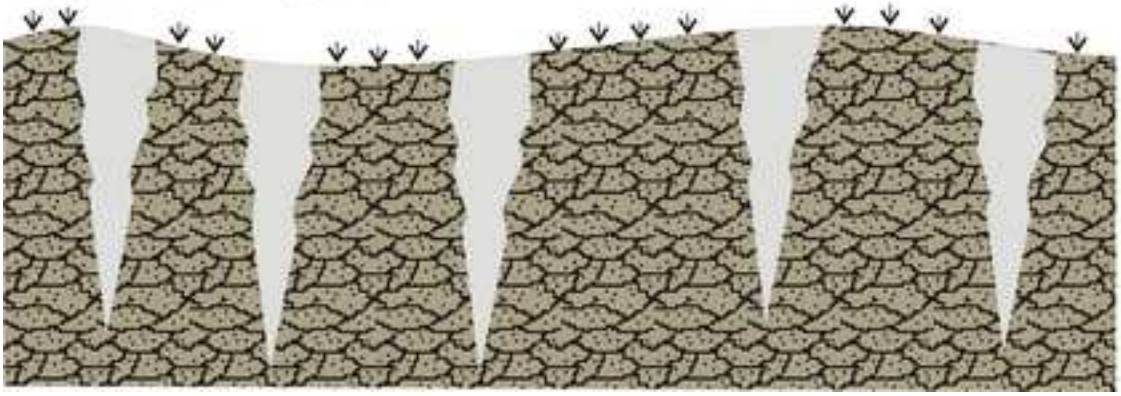

Table 1 Synopsis of the stratigraphic units exposed on the Dmitry Laptev Strait. The stratigraphical position of the Bychchagy Suite (grey highlighted) is still unclear

№	Period*	Characteristics	Name	Selected references
8	Holocene	Lacustrine and boggy deposits	Alas Sequence	Andreev et al. (2008)
7	Late (Sartan*), middle (Kargin), and early (Zyryan) Weichselian	Ice Complex deposits	Yedoma Suite	Nagaoka et al.(1995), Andreev et al. (2004, 2008), Nikolsky and Basilyan (2004)
6	Eemian (Kazantsevo)	Lacustrine and boggy deposits	Krest Yuryakh Suite	Andreev et al. (2004), Nikolsky and Basilyan (2004), Ilyashuk et al. (2006), Kienast et al. (2008)
5	Pre- or post-Eemian	Ice-rich deposits of controversial stratigraphic position	Bychchagy Suite	Tumskoy and Basilyan (2006)
4	Late Saalian (Taz)	Well-sorted flood plain deposits	Kuchchugui Suite	Andreev et al. (2004)
3	Middle Saalian (Shirta)	Palaeo active layer	Zimov'e Strata	Tumskoy and Basilyan (2006)
2	Middle Saalian (Shirta)	Ice Complex deposits	Yukagirsky Suite	Arkhangelov et al. (1996), Schirrmeister et al. (2002a), Andreev et al. (2004), Tumskoy and Basilyan (2006)
1	(?)	Late Cretaceous to Palaeocene periglacial reworked weathering crust	Cryogenic eluvium	Romanovskii and Hubberten (2001), Andreev et al. (2004)

* Local stratigraphic terms are given in parentheses according to Velichko et al. (2005)

Table 2 AMS-measured radiocarbon ages of plant remains in samples of the Alas sequences from Bol'shoy Lyakhovsky (L7-08) and Oyogos Yar (Oy7-11)

Sample №	Lab №	Altitude [m, a.s.l.]	Uncal. AMS ages [yr BP]		Cal. AMS ages* [yr BP], maximum	Cal. AMS ages* [yr BP], minimum
L7-08-25	KIA 36692	10.7	3960	±140	4830	4083
L7-08-22	KIA 35227	10.0	7525	±40	8309	8293
L7-08-19	KIA 35226	9.0	11610	+690/-640	15497	11755
L7-08-18	KIA 36691	8.4	10090	±150	12184	11223
L7-08-16	KIA 35225	7.9	9220	+190/-180	10890	9894
L7-08-14	KIA 36690	7.5	7095	±60	8020	7794
L7-08-12	KIA 35224	6.8	11210	+880/-800	15378	10650
L7-08-08	KIA 35223	5.7	11860	±160	14050	13362
L7-08-05	KIA 35222	5.0	46620	+1750/-1440		
L7-08-02	KIA 36689	4.2	44030	+820/-750		
Oy7-11-14	KIA 35234	11.1	3325	±35	3635	3477
Oy7-11-12	KIA 35233	10.1	8335	±45	9472	9247
Oy7-11-10	KIA 35232	8.8	8260	±40	9408	9092
Oy7-11-09	KIA 36687	8.6	9985	±35	11616	11271
Oy7-11-08	KIA 36686	8.3	11145	±40	13141	12943
Oy7-11-07	KIA 35231	8.0	14830	+70/-60	18500	17731
Oy7-11-06	KIA 36688	7.7	10720	+40/-35	12839	12700
Oy7-11-04	KIA 35230	7.1	11995	±50	13984	13748
Oy7-11-03	KIA 35229	6.8	41290	+2370/-1830		
Oy7-11-01	KIA 35228	6.0	36580	+1090/-960		

*Calibrated ages were calculated using the software program „ CALIB rev 5.01"
(Data set: IntCal04; Reimer et al. 2004)

Table 3 Oxygen and hydrogen stable isotope signatures (mean values and standard deviations) of post-Eemian Glacial and Holocene ice wedges (IWs)

Type of ground ice	Sub-samples	Altitude	$\delta^{18}O$ mean	$\delta^{18}O$ σ	δD mean	δD σ	*d* mean	*d* σ
		[m a.s.l.]	[‰]	[‰]	[‰]	[‰]	[‰]	[‰]
Holocene IW (syngenetic)	11	11	−23.63	1.35	−181.8	10.2	7.3	1.2
Holocene IW (epigenetic)	2	6.5	−19.87	1.96	−158.4	13.4	0.5	2.2
Post-Eemian IW (syngenetic)	8	8.5	−28.62	0.25	−218.3	1.3	10.7	0.8

Table 4 Taxonomic reference list of all identified ostracod species from Eemian and Late Glacial/Holocene deposits

Ostracod taxa	
Candona candida	(O.F. MÜLLER, 1776)
Candona cf. neglecta	SARS, 1887
Fabaeformiscandona harmsworthi	(SCOTT, 1899)
Fabaeformiscandona levanderi	(HIRSCHMANN, 1912)
Fabaeformiscandona rawsoni	(TRESSLER, 1957)
Fabaeformiscandona tricicatricosa	(DIEBEL & PIETRZENIUK, 1969)
Limnocythere falcata	DIEBEL, 1968
Limnocythere suessenbornensis	DIEBEL, 1968
Limnocytherina sanctipatricii	(BRADY & ROBERTSON, 1869)
Cytherissa lacustris	(SARS, 1863)
Cypria exsculpta	(FISCHER, 1855)
Cyclocypris laevis	(O.F. MÜLLER, 1776)
Eucypris dulcifons	DIEBEL & PIETRZENIUK, 1969
Ilyocypris lacustris	KAUFMANN, 1900
Tonnacypris glacialis	(SARS, 1890)

Table 5 Oxygen and carbon stable isotope signatures (mean values, maxima and minima) of ostracod calcite from different periods

Site	Uncal. ages [kyr BP]	№ of sub-samples	Species	$\delta^{18}O$ mean [‰]	$\delta^{18}O$ max [‰]	$\delta^{18}O$ min [‰]	$\delta^{13}C$ mean [‰]	$\delta^{13}C$ max [‰]	$\delta^{13}C$ min [‰]
North Yakutia*	modern	1	*C. candida*	−14.97	--	--	−6.91	--	--
Central Yakutia**	modern	6	*C. candida* / *C. muelleri-jakutica*	−10.34	−8.88	−11.64	−1.96	0.24	−5.75
L7-08	11.6 to 10.1	8	*C. candida*	−13.37	−12.34	−15.12	−5.62	−4.23	−7.40
		10	*C. lacustris*	−14.10	−13.03	−14.89	−7.54	−6.28	−9.93
R33 A1***	12.5	21	*C. candida*	−12.99	−12.21	−13.93	−6.13	−5.29	−6.77
		19	*C. lacustris*	−14.01	−12.82	−14.86	−7.82	−6.04	−9.77
Oy7-08	Eemian	5	*C. candida*	−11.70	−11.25	−12.59	−5.05	−4.70	−5.50
		8	*C. lacustris*	−13.08	−12.15	−14.48	−8.53	−7.28	−10.2

*Wetterich et al. (2008b); **Wetterich et al. (2008a); ***Andreev et al. (2009)